Artemisia Annua Extracts Improve the Cognitive Deficits and Reverse the Pathological Changes of Alzheimer's Disease via Regulating YAP Signaling

Wenshu Zhou
Bingxi Lei
Chao Yang
Marta Silva
Xingan Xing
Wenhua Zheng (wenhuazheng@um.edu.mo)

Research Article

Keywords: Alzheimer's disease, Artemisia annua extracts, Neuronal apoptosis, AD-type pathologies, YAP signaling pathway

Posted Date: February 15th, 2022

DOI: https://doi.org/10.21203/rs.3.rs-1353187/v1

Abstract

Background: Alzheimer's disease (AD) is a chronic neurodegenerative disease characterized by a progressive loss of memory and cognitive functions, language disorders, functional and behavioral alterations. The neurotoxicity is associated with the aggregation of β-amyloid (Aβ) plaques and the downstream pathologies events such as Tau hyperphosphorylation, oxidative stress, neuroinflammation, and mitochondrial dysregulation play critical roles in the development of AD. With no effective treatment available for the prevention and treatment of AD, the search for new therapies has become the focus of many researchers.

Methods: *Artemisia annua* extracts were extracted and a water-soluble *artemisia annua* extract (*Ex1*) was used in treatment for 3xTg AD mice via oral administration. Cognitive functional recovery, Aβ accumulation, hyper-tau-phosphorylation, and the release of inflammatory factors and apoptosis were assessed three months after the treatment. In vitro, PC12 cells were incubated with 8 μM $A\beta_{1\text{-}42}$ with or without *Ex1* at different concentrations for 24h. ROS levels, mitochondrial membrane potential, caspase-3 activity, neuronal cell apoptosis, inflammation, and the phosphorylation of Tau, as well as involvement in the signaling pathway, were assessed by using biological technology.

Results: Oral administration of *Ex1* to AD 3xTg mice significantly improved the cognitive deficits, reduced Aβ accumulation, hyper-tau-phosphorylation, and the release of inflammatory factors and apoptosis. *Ex1* promoted the survival and proliferation of neural progenitor cells (NPS), increased the expression of synaptic proteins and neuronal cell survival. Similarly, *Ex1* significantly reversed the Aβ1-42-induced increase of ROS levels, caspase-3 activity, neuronal cell apoptosis, inflammation, and the phosphorylation of tau in vitro.

Conclusions: These findings suggest that *a water-soluble artemisia annua extract (Ex1)* may be a new multi-target anti-AD drug with potential use in the prevention and treatment of Alzheimer's disease.

Background

Alzheimer's disease (AD) is a chronic neurodegenerative condition with a worldwide incidence continuously increasing [1]. Characterized by a continuing memory loss and cognitive impairment, language disorders, functional and behavioural alterations, it has a dramatic bearing on patients' quality of life [2]. Despite the increasing understanding of AD pathophysiology, so far no effective drug has been proved successful against it, with available therapies failing to treat or prevent the disease progression[3]. AD pathological changes comprehend the presence of extracellular amyloid-β (Aβ) plaques and intracellular neurofibrillary tangles (NFTs) comprised of hyperphosphorylated microtubule-associated *tau* protein [4]. The overproduction and aggregation of Aβ peptides in AD brains have been reported to prompt a series of pathological occurrences that lead to tau hyperphosphorylation, increased oxidative stress, mitochondrial dysregulation, microglial and astrocytic activation, ultimately resulting in neuronal and synaptic loss, and in a significant atrophy in brain areas involved in the regulation of the cognitive

function. Intracellular NFTs compromise both neuronal and synaptic functions and its extent and distribution have been reported to correlate with the duration and severity of AD [5].

Neurogenesis, comprising both the proliferation of neural stem or progenitor cells and the differentiation of neurons, is a long term process responsible for maintaining the normal function of the central nervous system (CNS) [6]. Neurogenesis impairment in the brains of adult mice has been associated with learning and memory deficits, and other cognitive alterations [7, 8]. In a recent study, analysis of AD brains revealed a progressive decline of neurogenesis as the disease progressed in comparison with the brains of neurologically healthy individuals. Importantly, this decline manifests at early stages of the disease, before the presence of Aβ plaques and NFTs [9]. Therefore, the development of therapeutic strategies aiming to enhance adult neurogenesis could stand as promising novel treatment strategies to tackle AD.

The Hippo pathway is an evolutionary conserved kinase cascade, whose main components include the mammalian sterile 20-like 1/2 (MST1/2), large tumor suppressor homolog 1/2 (LATS1/2), MOB kinase activator 1A/B (MOB1A/B), and Yes-associated protein (YAP)/Transcriptional co-activator with PDZ binding motif (TAZ) [10-13]. Numerous evidence suggest that these components, especially YAP, have a key role in organ development and tissue homeostasis via regulation of cellular behaviors such as cell proliferation, survival, apoptosis, migration, and differentiation [14, 15]. Hippo signaling also controls stem cells self-renewal, proliferation and differentiation, triggering the regeneration of tissue [16, 17]. Upon activation, MST1/2 kinase undergoes autophosphorylation and activates LATS1/2 and MOB1. LAST1/2 activation triggers the phosphorylation of YAP Ser127 promoting its cytoplasmatic retention and proteolytic degradation in a 14-3-3 protein-dependent manner [18]. Contrarily, inactivation of MST1/2 enables unphosphorylated YAP to translocate to the nucleus and bind to the TEA domain family (TEADs) transcriptional factors, triggering the transcription of genes involved in a series of biological occurrences, including cellular growth, proliferation, and survival [19, 20]. Many of these biological events are mapped with those involved in the pathogenesis of AD. In fact, the hyperactivity of Hippo cascade has been reported to be connected to Aβ-induced neuron death and amyloid precursor protein (APP) signaling in AD [21].

Artemisia annua herb has been used for more than 2000 years in traditional Chinese medicine being attributed different important biological properties including anti-malarial [22], anti-tumor [23, 24], anti-inflammatory [25-28], antibacterial [29], antioxidant and immunoprotected effects [30-32]. Importantly, *Artemisia annua* is non-toxic and harmless within a certain dose range [33], with several studies reporting its potential therapeutic use [34, 35]. It contains several biologically active ingredients, such as sesquiterpene lactones (artemisinin), flavonoids, polysaccharides, coumarins, volatile oils and phenolic compounds known as phenols. Among these, artemisinin has been the most extensively studied due to its widely recognized anti-malarial properties [36]. More recently, researchers reported the neuroprotective effect of artemisinin and its derivatives and their prospective use in the treatment of different neurodegenerative diseases [37, 38]. Artemisinin was shown to be able to promote neural stem/progenitor cells differentiation into NeuN(+) neurons [29], and evidence that artemisinin is able to suppress YAP signal transduction have also been reported [30], with studies suggesting that YAP controls

neural progenitor number [31], self-renew [32], and neurogenesis [33]. Based on these findings, we speculated that *artemisia annua* might exhert a neuroprotective effect that may be potentiated by the diversity and richness of its bioactive compounds, and this effect might be modulated via regulation of YAP signaling. Therefore, in this study, we intended to assess the protective effect of *artemisia annua* extract on AD and the potential underlying mechanisms of action. Obtained results showed that a water soluble *artemisia annua* extract *Ex1*, selected among 3 other *artemisia annua* extracts tested, reliefed AD symptoms and reversed the pathological changes of AD *in vitro* and *in vivo* via activation of the YAP pathway.

Methods

Extracts from Artemisia annua preparation

Dried *extracts* from *artemisia annua* were obtained from Nanjing Puyi Biotechnology company. The extraction process was performed as follows: *Artemisia annua* water-soluble *Ex1* extracts were obtained by soaking *artemisia annua* dried powder in distilled water (1:10) wt./vol for 2 hours and then heated and boiled for additional 2 hours (primary extraction). The extract was then filtered, soaked again in distilled water (1:8) wt./vol and left boiling for 1.5 hours (secondary extraction). After filtration, the extracting solutions were evaporated at 65°C under reduced pressure (-0.08 MPa), followed by lyophilization to obtain a relative density of 1.12. *Artemisia annua Ex2* and *Ex3* extracts were obtained, following the same methodology, by soaking *artemisia annua* dried powder in 55% and 75% ethanol, respectively.

Animals and treatment

3xTg transgenic mice (APPSWE, TauP301 L and PS1M146V) were obtained from the Jackson Laboratory and bred in the animal facility of the University of Macau. All animal experiments were approved by the University of Macau Animal Ethics Committee (protocol No. UMAEC-001-2020). The animals were housed in 24-26°C room, 12 hours/dark-light cycle and food and water were available *ad libitum.* Animals were randomly divided into four groups: Wild-type (WD, Ctrl), 3xTg (Ctrl), 3xTg+6.7 mg/ml *artemisia annua* and 3xTg+20 mg/ml *artemisia annua* groups (n=10 animals per group, female, ~30g, aged 9 months). Animals from 3xTg+6.7 mg/ml group and 3xTg+20 mg/ml group were treated with *artemisia annua* extracts dissolved in the drinking water. Animals from the WT and 3xTg groups received equal amounts of water. After 3 months of treatment the behavioral performance of all mice was examined by Morris water maze.

Behavioral Tests

Morris water maze (MWM) test was used to analyze the effect of *artemisia annua* extracts on the memory and learning abilities of mice according to previously described methods [39-41]. Briefly, the animals were submitted to a place navigation test during 5 consecutive days, followed by a spatial probe trial on the sixth day. During the place navigation tests the platform was placed in the middle of one of the quadrants and 1 cm above the water surface. The path distance and latency of finding the platform

were tested and used as indicators of the mice learning ability. On the day of spatial probe trial, the mice searched the platform for 60 s, which had been previously removed. The time spent in the target quadrant and the number of crossings was measured. All data acquisition and processing were done by image analyzing software (ANY-maze; Stoelting). Before the Morris water maze test, the swimming abilities of all mice were assessed with mice unable to swim being excluded from the study.

Tissue samples preparation

All mice were euthanized using chloral hydrate (0.25 mg/ml) and the brains were dissected and fixed in 4% paraformaldehyde (4% PFA) for 48 h at 4℃. After fixation, some of the samples were dehydrated and embedded in OCT, and kept at -20 °C until further analysis. Other samples were put into 75% alcohol, dehydrated and embedded with paraffin (Leica, EG1150), and kept at 4 °C until further analysis.

Immunofluorescence analysis

For immunofluorescence, the brains were cut into 20 μm slices using a low temperature thermostat. After incubation with 0.2% Triton X-100 (Gibco) for 30 mins, the sections were washed with PBS and incubated with blocking buffer composed of 3% BSA (Sigma-Aldrich, A9647) in PBS for 30 min at room temperature. The samples were then incubated with primary antibodies overnight at 4°C: SOX2 (Millipore, MAB5603, 1:400), BrdU (Bu20a) mouse mAb (CST, 5292, 1:500), NESTIN (Millipore, MAB5922, 1:400), MAP2 (Millipore, MAB1637,1:400), GFAP (CST, G9269, 1:600), Iba1 (GeneTex, GTX10042, 1:400), Phospho-Tau (Thr181) (CST, D9F4G, 1:500), Anti-Tau (phospho S396) (Abcam, ab109390, 1:400), β-Amyloid, Mouse (6E10) (BioLegend, 803004, 1:500), YAP (Santa cruz, SC-101199, 1:1000), p-YAP(Ser127) (CST, 4911s, 1:1000), TAZ (CST, 83669, 1:1000), Bcl2 (CST, 32012, 1:1000), Bax (CST, 34260-2, 1:1000), caspase 3 (CST, 1:1000), cleaved caspase 3 (CST, 1:1000), MST1(SCT, 3682,1:1000); Mst1 (Phospho-Thr183) (ASB, 12144, 1:1000); LATS1(CST□3477,1:1000), LATS1 (Phospho-Ser909) (SAB, 13033,1□500)□ MOB1(CST, 13730,1□1000), Phospho-MOB1 (Thr35) (CST, 8699,:1000), Survivin (SAB, 24092,1:1000),PML(SAB, 32211,1:1000), and GAPDH (CST, 3683s, 1:1000). In the next day, the samples were rinsed with PBS and incubated for one hour at room temperature with the corresponding secondary antibody (Alexa Fluor 488 anti-mouse or 594 anti-rabbit (Invitrogen, 1: 500)). The sections were blocked by anti-fluorescence quenching blocking solution with DAPI, then analyzed and photographed using a microscope (Carl Zeiss Confocal, LSM710). All studies were performed three times, with 10 animals in each group.

Cells culture and treatments

PC12 and SH-SY5Y cells were cultured in Dulbecco's Modified Eagle Medium (DMEM) supplemented with 10% fetal bovine serum (FBS) and 0.1% penicillin/streptomycin and incubated at 37 °C with 5% CO_2 humidified atmosphere. The medium was changed every 2–3 days, and the cells were sub-cultured when reaching 80–90% confluency using 0.25% trypsin. After digestion, the cells were centrifuged at 1000 rpm for 3 min and resuspended in fresh medium.

Primary neuronal cells were isolated from C57BL/6 mice brains and cultured in neuronal culture medium, as previously described [42]. Briefly, newborn C57BL/6 mice, obtained from the animal facility of the University of Macau, were sacrificed and the brain was surgically removed and washed with cold PBS to remove all the blood. Brain homogenates were digested with 0.25% trypsin for 10 min at 37℃. Obtained cell suspension was filtered through a 0.45μm pore size filter unit, centrifuged at 1000xg for 5 min, and the supernatant removed. Obtained cells were seeded in poly-D-lysine plates with neurobasal medium containing 1% B27, 1% N2, 1% NEAA and 50μM glutamine.

CRISPR/Cas9 genome editing

CRISPR/Cas9 sgRNA targeting YAP (ATACCCTTACCTGTCGCGAG) was designed using Crispr design online tool (http://www.genome-engineering.org/crispr/). The sgRNA oligo primer was synthesised by BGI, China. After that, sgRNA was cloned into the pSpCas9(BB)-2A-Puro (PX459) V2.0 sequence (Addgene plasmid #62988) from Feng Zhang lab[43]. The presence of the insert was verified by isolating the plasmid DNA from several bacterial colonies and performing sequencing from the U6 promoter (human) (CCGTAACTTGAAAGTATTTCG). Isolated plasmid from positive colonies was transfected into PC12 cells using Lipofectamine 3000 according to the manufacturer's instructions (Thermo Fisher). The cells were sorted out using 2.5ug/ml puromycin and cultured into single colonies in 96-well plates. YAP expression in WT and KO cells was assessed by western blot.

MTT assay

The cell viability was assessed using MTT assay as previously described [44, 45]. Briefly, the cells were seeded in 96-well plates at a density of 5×10^3 cells/well in complete medium. In the following day, seeded cells were incubated for 24 hours with: (1) different concentrations of *artemisia annua* extracts; (2) different concentrations of $A\beta_{1\text{-}42}$ and (3) $A\beta_{1\text{-}42}$ with or without different concentrations of *artemisia annua* extracts. After the treatment, cells were further incubated with MTT (0.5 mg/ml) for additional 3-4 hours, and the medium was replaced with 100 μl DMSO to dissolve the blue formazan crystals formed by live cells. The absorbance was measured at 570 nm using a microplate reader (SpectraMax 250, Molecular Device, Sunnyvale, CA, USA). Cell viability was calculated as a percentage of the control group.

Measurement of reactive oxygen species (ROS)

The levels of intracellular ROS were tested using Cell ROXs Deep Red Reagent (Thermo Fisher Scientific, USA), according to the protocol provided by the manufacturer. After appropriate treatment, the cells were kept in the dark with CellROXs Deep Red Reagent (5 mM) in DMEM (without FBS) for 30 min and washed twice with phosphate buffered saline (PBS) solution. The fluorescence was measured with an Infinite M200 PRO Multimode Microplate using an emission wavelength of 665 nm and an excitation wavelength of 640 nm.

Measurement of mitochondrial membrane potential (△ψm)

The mitochondrial membrane potential (△ψm) was measured by JC-1 assay, according to the protocol provided by the manufacturer. After appropriate treatment, the cells were incubated with 1x JC-1 (10 μg/ml in medium without FBS) at 37°C for 30 min and washed two times with PBS solution. The intensities of red fluorescence (excitation 560 nm, emission 595 nm) and green fluorescence (excitation 485 nm, emission 535 nm) were measured using an Infinite M200 PRO Multimode Microplate. The ratio of JC-1 red/green fluorescence intensity was used to calculate the △ψm. All the values were normalized to the control group.

Caspase 3 activity assay

The levels of caspase 3 were measured using a caspase 3 activity assay kit (C1115, Beyotime Institute of Biotechnology, Shanghai, China). After 24 h of treatment, the cells were digested with 0.25% trypsin at 37℃ for 1 min, collected and centrifuged at 500x g for 5 min at 4 °C. The supernatant was then removed and the cells were washed once with PBS solution. Following the manufacturer's instructions, 100 μL of lysis buffer were added per two million cells. Cells were then lysed for 15 min on ice followed by centrifugation at 12000xg for 15 min at 4°C. Afterwards, 40 μL of the detection buffer and 10 μL of Ac-DEVD-pNA (2 mM) were added to 50 μL of each sample. Obtained solutions were mixed carefully avoiding the production of bubbles and incubated for 60-120 min at 37°C. The production of pNA was measured by the absorbance values at 405 nm using an Infinite M200 PRO Multimode Microplate. Caspase-3 activity results were normalized to the control group.

TUNEL assay

TUNEL staining was used to test cellular apoptosis, according to the instructions provided by the manufacturer (C1090, Beyotime, Shanghai, China). Briefly, after appropriate treatment, the cells were washed two times with PBS, and fixed in 4% paraformaldehyde (PFA) for 30 min. The cells were then washed one time with PBS, incubated with 0.3 % Triton X-100 in PBS for 10 min at room temperature, rinsed once with PBS, followed by incubation with 0.3 % H_2O_2 in PBS for 30min. After this period the cells were incubated with 50 μl of TUNEL reaction mixture (5 μl of TdT enzyme and 45 μl of fluorescent labeling solution) for 60 min at 37℃ protected from light. TUNEL-positive cells (green fluorescence) were observed under a fluorescent microscope and counted. The apoptosis was calculated as a percentage of the total number of cells. For tissue samples the same methodology was used.

Flow cytometry

Flow cytometric assay was performed following the instructions provided by the Sangon Biotech manufacturer (REF:E606336-0100). Briefly, after appropriate treatment the cells were harvested and centrifuged at 1000 rpm for 5 min. The cells were rinsed twice with ice-cold PBS and resuspended in Annexin V-FITC/PI binding buffer (195 μL). Annexin V-FITC (5 μL) was added and the cells were kept in the dark at room temperature for 30 min. Cells were then centrifuged at 1000 rpm for 5 min and re-suspended in Annexin V-FITC/PI binding buffer (190 μL). Propidium iodide (PI) (10 μL) was further added

and allowed to incubate in the dark for 5 mins. The quantification of apoptotic cells was performed using flow cytometry analysis.

Western blot

Western blot was performed to assess the expression levels of molecules or enzymes involved in Aβ production and degradation, Tau phosphorylation, oxidative stress, synapse-related proteins, apoptosis-related proteins, and hippo pathway-associated proteins. Protein samples from cultured cells and brain homogenates were successfully extracted with RIPA buffer and quantified using the BCA assay kit (Thermo Fisher, 23225). After electrophoresis, the proteins were transferred to 0.22 μm PVDF membranes for 1.5 hours. The blotted PVDF membranes were blocked for 2 h with 5% BSA (TBST) and incubated with the primary antibodies (1:1000) at 4°C overnight. After washing with TBST (3 times, 10 min each), the membranes were incubated for 2 h with the secondary antibody (1:5000) at room temperature. Enhanced chemiluminescent was used to detect the blots.

Statistical analysis

Statistical analysis was performed using GraphPad Prism 5 software. All results are expressed as the mean ± SEM from three experiments. The statistical significance between multiple groups was determined using one or two-way ANOVA followed by Tukey's post-hoc test. $p < 0.05$ was considered statistically significant.

Results

Artemisia annua extracts improved the cognitive deficits of 3xTg AD mice.

The potential of the different *artemisia annua* extracts obtained via different techniques (refer to the methods section) to improve the cognitive functions of 3xTg AD mice was assessed by Morris Water Maze (MWM) test. Obtained results showed that 3xTg AD mice treated with the different *artemisia annua* extracts for 3 months performed better than untreated 3xTg AD mice (Supplementary Fig. S1). According to these preliminary results, *artemisia annua* water-soluble extracts (*Ex1*), in comparison with the 55% and 75% ethanol extracts *Ex2* and *Ex3*, had a stronger therapeutic effect on mice treated with 6.7 mg/ml and 20 mg/ml doses (Supplementary Fig. S1-A). Therefore, *Ex1* was used in the subsequent *in vivo* experiments whose results showed that oral intake of *Ex1* improved the behavioral performance of 3xTg AD mice in comparison with untreated animals. Specifically, treated animals exhibited significant reductions in the escape latency (**Fig. 1A-B**) denoting an improvement of their cognitive functions. Importantly, the escape latency of treated animals was similar to WT animals from the control group. *Ex1* treatment also promoted a significant increase of the number of platform crossings and of the percentage of time spent on the target quadrant (**Fig. 1C-E**). These findings are indicative of the potential of *artemisia annua* extracts to recover the learning and memory deficits of the 3xTg AD mice experimental model.

Ex1 reduced Aβ accumulation in 3xTg AD mice

Analysis of the effect of *Ex1* on Aβ accumulation, revealed that mice treated with *Ex1* exhibited lower Aβ deposition in the brain cortex and hippocampus than untreated animals, as evaluated by IF. Interestingly, the effect of *Ex1* on Aβ deposition was higher in animals treated with lower concentrations of the extracts (**Fig. 2A**). Further analysis of the expression of the amyloid precursor protein (APP) and $A\beta_{1-42}$ in brain homogenates by western blot, revealed that APP expression levels were significantly reduced in treated 3xTg AD mice in comparison with untreated 3xTg AD animals and, once again, this effect was more evident in the group treated with a lower *Ex1* dose (**Fig. 2B-D**).

Ex1 reduced Tau-phosphorylation in 3xTg AD mice

Analysis of Tau phosphorylation showed that *Ex1* significantly improved Tau pathology (**Fig. 3**). Specifically, the fraction area of Tau-Thr181-positive neurons in the subregions of the hippocampus and cortex of 3xTg AD treated mice was significantly reduced in comparison with untreated mice (**Fig. 3A**). Moreover, mice receiving the dosage of 20 mg/ml exhibited a more pronounced reduction of tau-phosphorylation compared with animals treated with 6.7 mg/ml (**Fig. 3A**). Western blot analysis revealed that Tau-phosphorylation at different sites (Serine^{369} and Threonine^{182}) was significantly reduced in the brain of 3xTg AD mice treated groups. Interestingly, we also found that the animals treated with 20 mg/ml dose presented a more obvious decrease of Tau-phosphorylation (**Fig. 3B-C**). Still, the herbal extracts didn't affect the expression of total-Tau.

Ex1 attenuated neuroinflammation in 3xTg AD mice

Increasing evidence suggest that the occurrence of neuroinflammatory alterations, such as chronic microgliosis and astrogliosis, are crucial contributors to the progression of AD pathology [46]. Therefore, we evaluated the expression of Glial fibrillary acidic protein (GFAP, astrocytes marker) and Iba-1 (microglia marker) in the hippocampus and cortex. Obtained results indicate that the expression of GFAP was significantly increased in 3xTg AD mice in comparison with WT mice, being significantly reduced by *Ex1* treatment (**Fig. 4A**). Likewise, untreated 3xTg AD mice exhibited higher Iba-1 expression levels comparatively to WT mice, being reduced in both 6.7 mg/ml and 20 mg/ml treatment groups (**Fig. 4B**). To further support these findings, the levels of IL-1β, IL-6, TNF-α and IFN- γ were assessed by western blot. Compared with untreated 3xTg AD, mice in both 6.7 mg/ml and 20 mg/ml treatment groups showed a significant reduction of the expression levels of these inflammatory factors (**Fig. 4C-F**).

Ex1 promoted the proliferation of neural progenitor cells and increased the expression synaptic proteins in 3xTg mice via regulation of hippo signaling

Evidence suggests the occurrence of neurogenesis impairments in the AD. The decline of adult neurogenesis that accompanies AD progression has been associated with an aggravation of the cognitive deficits and its upregulation has been shown to improve cognition [47, 48]. Hence, the development of treatments able to enhance neurogenesis pose as a potential therapeutic approach to be

used in the treatment of AD. Immunofluorescence double-labeling of neuronal progenitor cells (NPs) with Sox2 and Brdu (marker of proliferative cells) in the cortex and hypothalamus showed a significative reduction of the number of $Sox2^+/Brdu^+$ positive cells in 3xTg AD mice compared with WD control animals (**Fig. 5A**). In contrast, 3xTg AD mice treated with *Ex1* exhibited a significative higher number of $Nestin^+/Sox2^+$ positive cells in the same brain areas (**Fig. 5A**). And the number of $Sox2^+$ and $Brdu^+$ double positive cells was determined, compared with untreated 3xTg AD mice, treated mice exhibited significant increased numbers of $Sox2^+$ and $Brdu^+$ positive cells in both 6.7 mg/ml and 20 mg/ml treatment groups (**Fig. 5B-C**), indicating that *Ex1* promoted the survival and proliferation of NPs in 3xTg AD mice. Further investigation of the effect of *artemisia annua* extracts in the dendritic loss exhibited by 3xTg AD mice, showed that both 6.7 mg/ml and 20 mg/ml doses of *Ex1* treatment promoted the upregulation of synapse-related proteins expression levels (**Fig. 5D-E**), indicating that *artemisia annua* extracts rescued the dendritic loss in the brains of 3xTg AD mice.

Ex1 rescued neuronal cell apoptosis in 3xTg AD mice via activation of Hippo/YAP signaling

Multiple evidence indicate that the transcription coactivators YAP/TAZ and TEAD of the Hippo signaling pathway play a critical role in the proliferation, survival, and metabolism of cells [17, 49-51]. Moreover, in a recent study, YAP was also implicated as a hub molecule in AD pathology [52]. Assessment of the effect of *Ex1* in the neuronal apoptosis of AD mice by TUNEL staining assay, indicates that the increased number of apoptotic cortical neurons in 3xTg AD mice was significantly decreased by *Ex1* treatment (**Fig. 5F-G**). These alterations were accompanied by changes in the expression of different apoptosis regulators including Bax, Bcl-2 and cleaved caspase 3 (**Fig. 6H-I**). Specifically, *Ex1* promoted the increase of Bcl-2/Bax ratio and the decrease of cleaved caspase 3 expression (**Fig. 6H**). Previous studies indicate the involvement of the Hippo signaling in the inhibition of apoptosis [20]. Activation of the Hippo signaling pathway triggers the functional inactivation of YAP and TAZ promoting the occurrence of cellular apoptosis [53-55]. Accordingly, the expression levels of YAP and TEAD2 were significantly increased in treated 3xTg AD mice compared with untreated 3xTg AD animals, while YAP phosphorylation levels were significantly decreased by *Ex1* treatment **(Fig. 5J-K**). Previous studies suggest that YAP interaction with TEAD transcription factors may result in the upregulation of anti-apoptotic genes such as survivin [56, 57]. On the other hand, phosphorylated YAP may also bind to p73 promoting the upregulation of pro-apoptotic genes, such as bax and promyelocytic leukemia (PML) [58-60]. In this study, *Ex1* treatment promoted a significant increase of survivin expression levels while significantly reducing the expression of PML (**Fig. 5L-M**). In addition, the phosphorylation levels of upstream MST1 and LATS1 proteins of the YAP signaling cascade were significantly decreased by *Ex1* treatment (**Fig. 5N-P**), while MOB1 expression was not significantly altered (**Fig.5Q-R**). These results indicate that *Ex1* reduction of brain neuronal apoptosis may occur via YAP/TEAD/survivin signaling.

Ex1 antagonized $A\beta_{1-42}$-induced neurotoxicity and increased the viability of neuronal cells in vitro

Aiming to assess the neurotoxic effect of $A\beta_{1-42}$ *in vitro*, PC12 cells were incubated with increasing concentrations of $A\beta_{1-42}$ for 24 hours. Cell viability results revealed that incubation with $A\beta_{1-42}$ had a

significant cytotoxic impact at a concentration of 8 µM resulting in the death of 50% of neuronal cells (**Fig. 6A**). The study of the potential protective action of *artemisia annua* against $A\beta_{1-42}$-induced toxicity was preceded by the evaluation of the effect of the different extracts against $A\beta_{1-42}$. Similarly to the results obtained *in vivo*, *Ex1* exhibited, in comparison with *Ex2* and *Ex3*, a stronger neuroprotective effect against $A\beta_{1-42}$ induced neurotoxicity, being the extract chosen for the subsequent *in vitro* experiments (Supplementary Fig.S2). Incubation of PC12 cells with different concentrations of *Ex1* (1-1000 µg/ml) did not induce cytotoxicity on neuronal cells (**Fig. 6B**). Incubation of PC12 cells with different concentrations of *Ex1* and 8 µM $A\beta_{1-42}$ for 24 hours revealed that the extracts increased the viability of cells in a dose dependent manner, starting at the concentration of 10 µg/ml (**Fig. 6C**). Similar results were obtained using human neuroblastoma SH-SY5Y cells and primary cortical neurons, in which *Ex1* dose-dependently protected these cells from $A\beta_{1-42}$-induced neurotoxicity (**Fig. 6D-E**). These results propose that *Ex1* has a strong inhibitory action against the neurotoxicity of $A\beta_{1-42}$ exerting a neuroprotective action.

Ex1 treatment alleviated $A\beta_{1-42}$-induced apoptosis and attenuated the pathologic changes triggered by Aβ1-42 in PC12 cells

Apoptosis is a key event in AD, with studies reporting that Aβ can directly trigger apoptotic neuronal death *in vitro* and *in vivo* [61, 62]. Moreover, evidence suggest the upregulation of several cell-death regulatory proteins in AD brains [63]. In this study, *Ex1* promoted the decrease of $A\beta_{1-42}$ -induced increase of PC12 cells apoptosis as shown in Figure 8. Incubation of PC12 cells with 8 µM $A\beta_{1-42}$ promoted a significative impairment of the mitochondrial function denoted by the decrease of $\triangle\psi m$ that was prevented by *Ex1* treatment (**Fig. 7A-B**). Further evaluation of ROS production revealed a significant increase of intracellular ROS levels induced by $A\beta_{1-42}$ that was reduced by *Ex1* treatment (**Fig. 7C-D**). In addition, the increase of caspase 3 activity (**Figure 7H)** and decrease of the expression ratio between the anti-apoptotic Bcl2 and pro-apoptotic Bax proteins promoted by $A\beta_{1-42}$ incubation , was reversed by *Ex1* treatment (**Fig. 7J-K**). Similar results were obtained using human neuroblastoma SH-SY5Y cells and primary neurons (Supplemwntary Fig. S3), suggesting that *Ex1* have a potent anti-oxidant effect.

Further study aimed to assess the potential of *Ex1* to attenuate AD pathologic changes including Aβ aggregation, tau-phosphorylation, and the release of pro-inflammation factors. Here, PC12 cells were incubated with 8 µM $A\beta_{1-42}$ with or without *Ex1* at different concentrations for 24h. Western blot results showed that *Ex1* reduced the release of pro-inflammatory factors interleukin (IL)-1β **(Fig. 7K-k1)**, tumor necrosis factor (TNF)-α(**(Fig. 7K-k2)**) and IL-6 induced by $A\beta_{1-42}$ (**Fig. 7K-k3**). *Ex1* also had an inhibitory effect on the upregulation of the β-site APP cleaving enzyme 1 (BACE1) in a dose-dependent *manner* (**Fig. K-k4**). Similarly, the phosphorylation of Tau triggered by $A\beta_{1-42}$ incubation was dose-dependently reduced by *Ex1* at different phosphorylation sites (**Fig. K, k4-k6**), indicating that *Ex1* has a potent treatment effect on anti-AD related pathological changes induced by $A\beta_{1-42}$.

YAP is involved in the protective effect of Ex1 in PC12 cells

Assessment of the potential involvement of the Hippo/YAP signaling on the protective effect of *Ex1* in PC12 cells, showed that *Ex1* treatment promoted a dose-dependent increase of YAP and a downregulation of YAP phosphorylation levels (**Fig. 8A-B**). ICC assay further confirmed that *Ex1* treatment promoted YAP nuclear translocation and a significant increase of its expression levels (**Fig 8C**). In addition, *Ex1* promoted the upregulation of TEAD2 expression in a dose-dependent manner while having no significant effect in TAZ protein with the exception of the 300mg/ml dose (**Fig. 8D-E**). Further study found that *Ex1* promoted the increase of MST1/p-MST1 and LAST1/p-LAST1 ratios while having no significant effect in MOB1/p-MOB1, which are located upstream of the YAP signaling cascade (**Fig. 8J-K**). *Ex1* treatment also promoted a dose-dependent increase of survivin expression and a decrease of PML (**Fig. 8L-M**), two downstream anti- and pro-apoptosis genes of YAP signaling, indicating that *Ex1* anti-apoptotic effect may occur, at least in part, via regulation of Hippo signaling. To investigate this hypothesis, we checked the alterations in the Hippo signaling upon incubation with $A\beta_{1-42}$ and treatment with *Ex1*. Obtained results showed a decrease of YAP expression upon $A\beta_{1-42}$ incubation that was gradually increased by 300 µg/ml *Ex1* treatment (**Fig. 8N-O**). In contrast, $A\beta_{1-42}$ promoted the upregulation of YAP phosphorylation that was attenuated by *Ex1* treatment while having no significant impact on TAZ (**Fig. 8N-O**). ICC assay further confirmed that *Ex1* promoted a significant increase of YAP expression and its translocation to the nucleus (**Fig.8R**). TEAD2 was significantly downregulated upon incubation with $A\beta_{1-42}$ and successfully rescued by *Ex1* treatment (**Fig 8P-Q**). In addition, the decrease of survivin and increase of PML expressions caused by $A\beta_{1-42}$ incubation was attenuated by *Ex1* treatment (**Fig 8P-Q**). $A\beta_{1-42}$ also promoted the upregulation of p-MST/MST1 and p-LAST1/LAST1 ratios and these were altered by *Ex1* treatment. No significant changes were identified on MOB1 of Hippo signaling (**Fig 8U-V**). These findings show evidence that *Ex1* is able to protect against $A\beta_{1-42}$-induced apoptosis via regulation of YAP signaling.

To further verify whether YAP is associated with the survival effect promoted by *Ex1* against $A\beta_{1-42}$-induced cell apoptosis, the cells were pretreated with verteporfin (a specific inhibitor of YAP) for 60 min at a concentration of 2.5 µM [55] followed by incubation with *Ex1* and $A\beta_{1-42}$ for 24 h. MTT assay results showed that verteporfin at a concentration of 1 µM blocked the neuroprotective action of *Ex1* against $A\beta_{1-42}$-induced neurotoxicity (**Fig. 9A**). Incubation of cells with verteporfin for 60 min prior to $A\beta_{1-42}$ alone or with *Ex1* prevented the recovery of the mitochondrial membrane potential (**Fig. 9B-C**) and the decrease of intracellular ROS levels promoted by *Ex1* (**Fig. 9D-E**). TUNEL staining and flow cytometry results showed that verteporfin also blocked the inhibitory effect of *Ex1* against $A\beta_{1-42}$-induced cell apoptosis (**Fig. 9F-I**). YAP knockout using Crispr Cas9 approache further confirmed the involvement of YAP signalling on *Ex1* neuroprotective effect. After confirmation of the successful knockout of YAP on PC12 cells by Western blot analysis (**Fig. 9J**), the cells were incubated with 8 µM $A\beta_{1-42}$ with or without *Ex1* for 24 hours. MTT assay results confirmed that the neuroprotective effect of *Ex1* was blocked in the KO cellular model (**Fig. 9K**), further validating the involvement of YAP signaling in the protective effects of *Ex1* against $A\beta_{1-42}$-induced toxicity.

Discussion

AD is a intricate multifactorial disease caused by an interaction between genetic and environmental factors [64]. Despite extensive research, there is still no effective treatment able to halt the development or progression of this disease whose worldwide incidence has been continuously increasing. Therefore, we propose that a therapeutic approach able to target multiple pathways to stop the different signaling cascades driving AD pathogenesis including Aβ aggregation, Tau phosphorylation, oxidative stress, and mitochondrial dysfunction, could pose as an effective strategy. *Artemisia annua*-derived compound artemisinin and its analogue artemether, have been associated with a broad spectrum of neuroprotective actions, holding encouraging prospects for future AD therapies [40, 65]. However, the potential therapeutic effect of *artemisia annua* on the cognitive impairments and pathological changes observed during AD are still not known. In the present study, we describe for the first time the potential of the *artemisia annua* extract *Ex1* to significantly improve 3xTg AD mice' cognitive deficits, reduce Aβ accumulation, hyper-tau-phosphorylation, and the release of inflammatory and apoptotic factors. Moreover, *Ex1* promoted the survival and proliferation of neural progenitor cells (NPs), increased the expression of synaptic proteins, and inhibited neuronal cell death while stimulating the activation of Hippo signaling pathway. In this study, we also report that *Ex1* was able to protect neuronal cells against the neurotoxicity induced by $A\beta_{1-42}$ by promoting cell survival, restoring the mitochondrial membrane potential loss, and inhibiting ROS overproduction. In addition, *Ex1* was able to attenuate $A\beta_{1-42}$-induced apoptosis, inflammation, and tau phosphorylation. It also stimulated the increase of YAP expression while decreasing YAP phosphorylation, suggesting the involvement of the Hippo signaling pathway in the mediation of its protective effects.

Transgenic 3xTg AD mice develop many of the AD hallmarks, including Aβ and tau pathology, neuroinflammation and cognitive deficits. In this study, oral administration of *Ex1* to 3xTg AD mice for 3 months significantly improved their learning and memory deficits as denoted by the increased escape latency, number of platform crossings and time spent on the target quadrant in the Morris water maze test. Further testing also revealed an important impact of the treatment on Aβ aggregation and tau hyperphosphorylation, by promoting a significative decrease of its expression levels in the cerebral cortex and hippocampus. Increasing evidence suggest that the occurrence of neuroinflammatory changes, including chronic microgliosis and astrogliosis are also key contributors to the progression of AD pathology [46]. As a resident immune cell of the central nervous system (CNS), microglia promotes Aβ clearance in the early stages of the disease hinder its progression [46]. However, microglia overactivation triggers the release of different pro-inflammatory factors, contributing to the installation of a neuroinflammatory state in AD brains [66]. Similarly, astrocytes also play a key role in AD progression with evidence suggesting the accumulation of reactive astrocytes around amyloid plaques contributing to scar formation [67-69]. Our results showed that *Ex1* promoted an improvement of the animals' neuroinflammatory state by inducing a significant decrease of astrocytes and microglia expression and ultimately impairing the release of different pro-inflammatory factors including IL-1β, IL-6, TNF-α.

The neurotoxicity of $A\beta_{1-42}$ has been widely reported with different studies describing the use of this peptide fragment in the development of AD *in vitro* experimental models [70]. In line with previous reports, the incubation of PC12 cells with increasing concentrations of $A\beta_{1-42}$ promoted a dose-dependent cytotoxic effect denoted by the decrease of cellular viability [71-73]. Treatment with *Ex1* efficiently suppressed $A\beta_{1-42}$ neurotoxicity by promoting the survival of different neuronal cells, including PC12 and SH-SY5Y cell lines and primary neurons. Further assessment of the damage induced by $A\beta_{1-42}$ incubation revealed the occurrence of mitochondrial membrane potential loss, increase of ROS production and apoptosis. Widely recognized as key players in the course of AD progression [74, 75], the occurrence of mitochondrial dysfunction, oxidative damage and apoptosis was prevented by *Ex1*. Moreover, it also prevented the upregulation of many of the pathological and pro-inflammatory markers promoted by $A\beta_{1-42}$ incubation. These findings provide evidence of *Ex1* potential treatment effect against AD using *in vivo* and *in vitro* experimental models.

Several core components of the Hippo signaling pathway, especially YAP, have been reported to play a crucial role in several diseases, being involved in the regulation of tumorigenesis, regeneration, and apoptosis in different tissues [76-78]. Studies reporting the role of the Hippo pathway in the nervous system have been gradually emerging [79] and YAP has been recently implicated as a hub molecule in AD pathology [52]. Likewise, this study, shows evidence of the targeting potential of this pathway in AD prevention and treatment. Assessment of the mechanisms underlying *Ex1* protective action against the occurrence of neuronal death *in vivo* revealed that it is mediated, at least in part, via regulation of YAP signaling. The brains of mice treated with the herbal extracts exhibited an accentuated decrease of the number of apoptotic cortical neurons and alterations in the expression of different apoptosis regulators including Bax, Bcl-2, cleaved caspase 3, survivin and PML. These changes were accompanied by an increase of YAP and TEAD2 expression and a decrease of phosphorylated YAP, MST1 and LATS1. Similarly, *in vitro* studies showed an upregulation of YAP expression and its nuclear translocation, a downregulation of YAP phosphorylation and an increase of TEAD2 expression that was dose-dependent. Incubation of PC12 cells with *Ex1* alone also promoted the increase of MST1/p-MST1 and LATS1/p-LAST1 ratios, the upregulation of survivin and the downregulation of PML. *Ex1* treatment also promoted a dose-dependent increase of Bcl-2/Bax ratio and a decrease of caspase 3 expression suggesting that *Ex1* control of the neuronal cellular apoptosis may occur, at least in part, via regulation of Hippo/YAP signaling. These findings are in line with a recent study reporting that Aβ sequesters YAP from the nucleus into cytoplasmic Aβ aggregates ultimately impairing its function and leading to necrosis [80]. Treatment of cells with *Ex1* attenuated these alterations as well as the increase of caspase 3 expression levels induced by $A\beta_{1-42}$. Inhibition of YAP expression using the inhibitor Verteporfin or CRISPR Cas9 approaches prevented the protective action of *Ex1* against $A\beta_{1-42}$-induced damage. Further studies showed that *Ex1* treatment attenuated $A\beta_{1-42}$-induced phosphorylation of YAP, the increased p-MST1/MST1 and p-LATS1/LATS1 ratios, the reduced expression of TEAD2 and survivin and the increased the expression of PML further validating the involvement of YAP signalling in *artemisia annua* action.

It has been documented that YAP signaling in Hippo pathway drives TEADs regulation of the senescence and numbers of neural progenitor cells [17]. These cellular behaviors play a key role in the maintenance of the neural network activity suggesting the Hippo-pathway as a potential novel target to treat neurodegenerative diseases such as AD. Surprisingly, *in vivo* results showed an increased survival and proliferation of NP cells in the cerebral cortex and hypothalamus of animals treated with *artemisia annua* extracts. The occurrence of neurogenesis impairment has been implicated in AD [7, 8, 81], suggesting the use of therapeutic approaches able enhance adult neurogenesis as potential treatment strategies. Besides its neurogenic effect, *Ex1* also attenuated the occurrence of dendritic loss by promoting the upregulation of synapse-related proteins expression. Taking these findings into account, we might speculate that the strong neuroprotective effect exerted by *artemisia annua* extracts is due to its dual function in attenuating AD pathological alterations and promoting neurogenesis. Importantly, this action may be a result of the synergistic action of *Ex1* main active components artemisinic acid, arteether, and deoxyartemisinin.

Conclusions

Our findings demonstrate that a water soluble *artemisia annua extract* (*Ex1*) can improve the cognitive deficits and reverse the pathological changes of AD *in vivo*. In addition, *Ex1* has potential neuroprotective effect on $A\beta_{1\text{-}42}$-induced neurotoxicity, characterized by reversed $A\beta_{1\text{-}42}$-induced increase of ROS levels, caspase-3 activity, neuronal cell apoptosis, inflammation, and the phosphorylation of Tau in vitro *in vitro*. Our study further clarified the underlying therapeutic mechanisms of *Ex1in vivo* and *invitro*. Although further researches are needed to elucidate the underlying beneficial ingredients of *Ex1*, we suggest the potential use of *Ex1* in AD therapy. Being able to target multiple key cascades leading to AD pathogenesis, including Aβ aggregation, tau phosphorylation, oxidative stress, mitochondrial dysfuntion and neuroinflammation, artemisia annua extracts hold great promising as a potential compound to be used in the development of novel AD therapies (**Fig. 10**).

Limitations

In the present study, we demonstrated that *artemisia annua* has very promising effect in treating AD However, there were still some possible limitations in our research. Firstly, it is well established that as a Chinese herb medicine, *artemisia annua* contains several biologically active ingredients, such as sesquiterpene lactones, flavonoids, polysaccharides, coumarins, volatile oils and phenolic compounds known as phenols. While many of these components are water insoluble we used only a water-soluble *extract* from *artemisia annua* (*Ex1*) in this study for testing the primary therapeutic effect on AD. Therefore, we need to further identify the underlying beneficial compounds of the *extract* via analysis of Chinese medicine ingredients. Futher researches may consider using single compound from *Ex1* to test their effect separately . In the future, we also consider that the application of *Ex1*as the Chinese medicinal formula to develop the new products for treationg or preventing AD. Secondly, we only elucidate the Yap signaling to regulate the functional recovery and pathological changes in AD. Considering the complexity

of the drug composition, these effects may be regulated by a multi-target manner. Thirdly, the pathogenesis of AD still need to be further explored. Although the toxicity of amyloid-beta is one of the central hypotheses, we only adopted $A\beta_{1-42}$ as a marker for Aβ pathology. Future researches may consider using other types of Aβ protein to explore whether exist difference for its underlying effect.

Abbreviations

Aβ - Amyloid-β

AD - Alzheimer's disease

APP - Amyloid precursor protein

CNS - Central nervous system

DMEM - Dulbecco's Modified Eagle Medium

Ex1 - Water solvable *artemisia annua* extract

Ex2 - 55% ethanol artemisia annua extracts

Ex3 - 75% ethanol artemisia annua extracts

FBS - Fetal bovine serum

LATS1/2 - Large tumor suppressor kinases

MST1/2 - Mammalian sterile 20-like kinases:

MTT - 3-(4,5-Dimethylthiazol-2-yl)-2,5-diphenyltetrazolium bromide

MWM - Morris water maze

NFT - Intracellular neurofibrillary tangle

NP - Neural progenitor cell

ROS - Reactive oxygen species

TAZ - PDZ-binding motif

TEAD - TEA domain family

YAP - Yes-associated protein

△ψm - Mitochondrial membrane potential

3xTg - 3xTg transgenic mice

Declarations

Ethics approval and consent to participate

The study was approved by the University of Macau Animal Ethics Committee (protocol No. UMAEC-001-2020).

Consent for publication

Not applicable.

Availability of data and materials

All data in this study are available from the corresponding author on reasonable request.

Competing interests

The authors declare that they have no competing interests.

Funding

This research was supported by National Natural Science Foundation of China (32070969), The Science and Technology Development Fund, Macau SAR (File No. 0127/2019/A3, 0113/2018/A3 and 0038/2020/AMJ), The Guangdong Provincial Funding Committee for Basic and Applied Fundamental Research (2022-Natural Science Foundation), University of Macau (File No. MYRG2018-00134-FHS and MYRG2020-00158-FSH).

Authors’ contributions

Wenhua Zheng conceived the idea. Wenshu Zhou, Bingxi Lei, Yang Chao, Xingan Xing performed the experiments. Wenshu Zhou and Marta Silva drafted the manuscript, analyzed the data, and designed the figures. All authors discussed the results and edited this manuscript. All authors read and approved the final manuscript.

Acknowledgements

The authors are grateful to UM-FHS and core facilities for the equipment and administrative support for this study, and also NSFC (32070969), The Science and Technology Development Fund, Macau SAR (File No. 0127/2019/A3, 0113/2018/A3 and 0038/2020/AMJ), The Guangdong Provincial Funding Committee for Basic and Applied Fundamental Research (2022-Natural Science Foundation), University of Macau (File No. MYRG2018-00134-FHS and MYRG2020-00158-FSH) for their support to the studies.

Authors' information

Affiliations

Center of Reproduction, Development & Aging, Faculty of Health Sciences, University of Macau, Taipa, Macau SAR, China and Institute of Translation Medicine, Faculty of Health Sciences, University of Macau, Taipa, Macau SAR, China

Wenshu Zhou, Bingxi Lei, Yang Chao, Marta Silva, Xingan Xing &Wenhua Zheng

Zhuhai UM Science & Technology Research Institute, Zhuhai, China

Wenhua Zheng

References

1. R.N. Kalaria, G.E. Maestre, R. Arizaga, R.P. Friedland, D. Galasko, K. Hall, J.A. Luchsinger, A. Ogunniyi, E.K. Perry, F. Potocnik, M. Prince, R. Stewart, A. Wimo, Z.X. Zhang, P. Antuono, Alzheimer's disease and vascular dementia in developing countries: prevalence, management, and risk factors, Lancet Neurol 7(9) (2008) 812-26.
2. F.M. LaFerla, K.N. Green, S. Oddo, Intracellular amyloid-beta in Alzheimer's disease, Nat Rev Neurosci 8(7) (2007) 499-509.
3. D.M. Holtzman, J.C. Morris, A.M. Goate, Alzheimer's disease: the challenge of the second century, Sci Transl Med 3(77) (2011) 77sr1.
4. M. Höltje, S. Djalali, F. Hofmann, A. Münster-Wandowski, S. Hendrix, F. Boato, S.C. Dreger, G. Grosse, C. Henneberger, R. Grantyn, I. Just, G. Ahnert-Hilger, A 29-amino acid fragment of Clostridium botulinum C3 protein enhances neuronal outgrowth, connectivity, and reinnervation, FASEB journal : official publication of the Federation of American Societies for Experimental Biology 23(4) (2009) 1115-26.
5. A. Serrano-Pozo, M.P. Frosch, E. Masliah, B.T. Hyman, Neuropathological alterations in Alzheimer disease, Cold Spring Harbor perspectives in medicine 1(1) (2011) a006189.
6. C. Zhao, W. Deng, F.H. Gage, Mechanisms and functional implications of adult neurogenesis, Cell 132(4) (2008) 645-60.
7. G. Gheusi, H. Cremer, H. McLean, G. Chazal, J.D. Vincent, P.M. Lledo, Importance of newly generated neurons in the adult olfactory bulb for odor discrimination, Proc Natl Acad Sci U S A 97(4) (2000) 1823-8.
8. C.D. Clelland, M. Choi, C. Romberg, G.D. Clemenson, Jr., A. Fragniere, P. Tyers, S. Jessberger, L.M. Saksida, R.A. Barker, F.H. Gage, T.J. Bussey, A functional role for adult hippocampal neurogenesis in spatial pattern separation, Science 325(5937) (2009) 210-3.
9. E.P. Moreno-Jiménez, M. Flor-García, J. Terreros-Roncal, A. Rábano, F. Cafini, N. Pallas-Bazarra, J. Ávila, M. Llorens-Martín, Adult hippocampal neurogenesis is abundant in neurologically healthy

subjects and drops sharply in patients with Alzheimer's disease, Nature medicine 25(4) (2019) 554-560.

10. E.H. Chan, M. Nousiainen, R.B. Chalamalasetty, A. Schäfer, E.A. Nigg, H.H. Silljé, The Ste20-like kinase Mst2 activates the human large tumor suppressor kinase Lats1, Oncogene 24(12) (2005) 2076-86.
11. Z.C. Lai, X. Wei, T. Shimizu, E. Ramos, M. Rohrbaugh, N. Nikolaidis, L.L. Ho, Y. Li, Control of cell proliferation and apoptosis by mob as tumor suppressor, mats, Cell 120(5) (2005) 675-85.
12. B. Zhao, X. Ye, J. Yu, L. Li, W. Li, S. Li, J. Yu, J.D. Lin, C.Y. Wang, A.M. Chinnaiyan, Z.C. Lai, K.L. Guan, TEAD mediates YAP-dependent gene induction and growth control, Genes & development 22(14) (2008) 1962-71.
13. M. Praskova, F. Xia, J. Avruch, MOBKL1A/MOBKL1B phosphorylation by MST1 and MST2 inhibits cell proliferation, Current biology : CB 18(5) (2008) 311-21.
14. A.W. Hong, Z. Meng, K.L. Guan, The Hippo pathway in intestinal regeneration and disease, Nature reviews. Gastroenterology & hepatology 13(6) (2016) 324-37.
15. V. Fu, S.W. Plouffe, K.L. Guan, The Hippo pathway in organ development, homeostasis, and regeneration, Current opinion in cell biology 49 (2017) 99-107.
16. A. Ramos, F.D. Camargo, The Hippo signaling pathway and stem cell biology, Trends in cell biology 22(7) (2012) 339-46.
17. A. Lavado, J.Y. Park, J. Paré, D. Finkelstein, H. Pan, B. Xu, Y. Fan, R.P. Kumar, G. Neale, Y.D. Kwak, P.J. McKinnon, R.L. Johnson, X. Cao, The Hippo Pathway Prevents YAP/TAZ-Driven Hypertranscription and Controls Neural Progenitor Number, Developmental cell 47(5) (2018) 576-591.e8.
18. B. Zhao, L. Li, K. Tumaneng, C.Y. Wang, K.L. Guan, A coordinated phosphorylation by Lats and CK1 regulates YAP stability through SCF(beta-TRCP), Genes & development 24(1) (2010) 72-85.
19. J. Cheng, S. Wang, Y. Dong, Z. Yuan, The Role and Regulatory Mechanism of Hippo Signaling Components in the Neuronal System, Frontiers in immunology 11 (2020) 281.
20. S.P. Wang, L.H. Wang, Disease implication of hyper-Hippo signalling, Open biology 6(10) (2016).
21. A. Swistowski, Q. Zhang, M.E. Orcholski, D. Crippen, C. Vitelli, A. Kurakin, D.E. Bredesen, Novel mediators of amyloid precursor protein signaling, Journal of Neuroscience 29(50) (2009) 15703-15712.
22. W.E. Ho, H.Y. Peh, T.K. Chan, W.S. Wong, Artemisinins: pharmacological actions beyond anti-malarial, Pharmacology & therapeutics 142(1) (2014) 126-39.
23. S.J. Lang, M. Schmiech, S. Hafner, C. Paetz, C. Steinborn, R. Huber, M.E. Gaafary, K. Werner, C.Q. Schmidt, T. Syrovets, T. Simmet, Antitumor activity of an Artemisia annua herbal preparation and identification of active ingredients, Phytomedicine : international journal of phytotherapy and phytopharmacology 62 (2019) 152962.
24. S. Alesaeidi, S. Miraj, A Systematic Review of Anti-malarial Properties, Immunosuppressive Properties, Anti-inflammatory Properties, and Anti-cancer Properties of Artemisia Annua, Electronic physician 8(10) (2016) 3150-3155.

25. L. Bai, H. Li, J. Li, J. Song, Y. Zhou, B. Liu, R. Lu, P. Zhang, J. Chen, D. Chen, Y. Pang, X. Liu, J. Wu, C. Liang, J. Zhou, Immunosuppressive effect of artemisinin and hydroxychloroquine combination therapy on IgA nephropathy via regulating the differentiation of CD4+ T cell subsets in rats, International immunopharmacology 70 (2019) 313-323.
26. D.P. Qin, H.B. Li, Q.Q. Pang, Y.X. Huang, D.B. Pan, Z.Z. Su, X.J. Yao, X.S. Yao, W. Xiao, Y. Yu, Structurally diverse sesquiterpenoids from the aerial parts of Artemisia annua (Qinghao) and their striking systemically anti-inflammatory activities, Bioorganic chemistry 103 (2020) 104221.
27. J. Jiao, Y. Yang, M. Liu, J. Li, Y. Cui, S. Yin, J. Tao, Artemisinin and Artemisia annua leaves alleviate Eimeria tenella infection by facilitating apoptosis of host cells and suppressing inflammatory response, Veterinary parasitology 254 (2018) 172-177.
28. W. Qiang, W. Cai, Q. Yang, L. Yang, Y. Dai, Z. Zhao, J. Yin, Y. Li, Q. Li, Y. Wang, X. Weng, D. Zhang, Y. Chen, X. Zhu, Artemisinin B Improves Learning and Memory Impairment in AD Dementia Mice by Suppressing Neuroinflammation, Neuroscience 395 (2018) 1-12.
29. W.S. Kim, W.J. Choi, S. Lee, W.J. Kim, D.C. Lee, U.D. Sohn, H.S. Shin, W. Kim, Anti-inflammatory, Antioxidant and Antimicrobial Effects of Artemisinin Extracts from Artemisia annua L, Korean J Physiol Pharmacol 19(1) (2015) 21-7.
30. X. Zhao, J. Fang, S. Li, U. Gaur, X. Xing, H. Wang, W. Zheng, Artemisinin Attenuated Hydrogen Peroxide (H(2)O(2))-Induced Oxidative Injury in SH-SY5Y and Hippocampal Neurons via the Activation of AMPK Pathway, Int J Mol Sci 20(11) (2019).
31. S. Li, S.C. Chaudhary, X. Zhao, U. Gaur, J. Fang, F. Yan, W. Zheng, Artemisinin Protects Human Retinal Pigmented Epithelial Cells Against Hydrogen Peroxide-induced Oxidative Damage by Enhancing the Activation of AMP-active Protein Kinase, Int J Biol Sci 15(9) (2019) 2016-2028.
32. M. Skowyra, M.G. Gallego, F. Segovia, M.P. Almajano, Antioxidant Properties of Artemisia annua Extracts in Model Food Emulsions, Antioxidants (Basel, Switzerland) 3(1) (2014) 116-28.
33. M.U. Eteng, A.O. Abolaji, P.E. Ebong, E.A. Brisibe, A. Dar, N. Kabir, M. Iqbal Choudhary, Biochemical and haematological evaluation of repeated dose exposure of male Wistar rats to an ethanolic extract of Artemisia annua, Phytotherapy research : PTR 27(4) (2013) 602-9.
34. X. Wan, H. Ahmad, L. Zhang, Z. Wang, T. Wang, Dietary enzymatically treated Artemisia annua L. improves meat quality, antioxidant capacity and energy status of breast muscle in heat-stressed broilers, Journal of the science of food and agriculture 98(10) (2018) 3715-3721.
35. Z.H. Song, K. Cheng, X.C. Zheng, H. Ahmad, L.L. Zhang, T. Wang, Effects of dietary supplementation with enzymatically treated Artemisia annua on growth performance, intestinal morphology, digestive enzyme activities, immunity, and antioxidant capacity of heat-stressed broilers, Poultry science 97(2) (2018) 430-437.
36. A. Septembre-Malaterre, M. Lalarizo Rakoto, C. Marodon, Y. Bedoui, J. Nakab, E. Simon, L. Hoarau, S. Savriama, D. Strasberg, P. Guiraud, J. Selambarom, P. Gasque, Artemisia annua, a Traditional Plant Brought to Light, International journal of molecular sciences 21(14) (2020).

37. X. Zhao, S. Li, U. Gaur, W. Zheng, Artemisinin Improved Neuronal Functions in Alzheimer's Disease Animal Model 3xtg Mice and Neuronal Cells via Stimulating the ERK/CREB Signaling Pathway, Aging and disease 11(4) (2020) 801-819.
38. Y. Zhao, Z. Long, Y. Ding, T. Jiang, J. Liu, Y. Li, Y. Liu, X. Peng, K. Wang, M. Feng, G. He, Dihydroartemisinin Ameliorates Learning and Memory in Alzheimer's Disease Through Promoting Autophagosome-Lysosome Fusion and Autolysosomal Degradation for Aβ Clearance, Frontiers in aging neuroscience 12 (2020) 47.
39. R. Baeta-Corral, L. Giménez-Llort, Persistent hyperactivity and distinctive strategy features in the Morris water maze in 3xTg-AD mice at advanced stages of disease, Behavioral neuroscience 129(2) (2015) 129-37.
40. S. Li, X. Zhao, P. Lazarovici, W. Zheng, Artemether Activation of AMPK/GSK3β(ser9)/Nrf2 Signaling Confers Neuroprotection towards β-Amyloid-Induced Neurotoxicity in 3xTg Alzheimer's Mouse Model, Oxidative medicine and cellular longevity 2019 (2019) 1862437.
41. H. Tian, N. Ding, M. Guo, S. Wang, Z. Wang, H. Liu, J. Yang, Y. Li, J. Ren, J. Jiang, Z. Li, Analysis of Learning and Memory Ability in an Alzheimer's Disease Mouse Model using the Morris Water Maze, Journal of visualized experiments : JoVE (152) (2019).
42. G. Giordano, L.G. Costa, Primary neurons in culture and neuronal cell lines for in vitro neurotoxicological studies, Methods in molecular biology (Clifton, N.J.) 758 (2011) 13-27.
43. L. Cong, F. Zhang, Genome engineering using CRISPR-Cas9 system, Methods in molecular biology (Clifton, N.J.) 1239 (2015) 197-217.
44. W. Zheng, C.M. Chong, H. Wang, X. Zhou, L. Zhang, R. Wang, Q. Meng, P. Lazarovici, J. Fang, Artemisinin conferred ERK mediated neuroprotection to PC12 cells and cortical neurons exposed to sodium nitroprusside-induced oxidative insult, Free radical biology & medicine 97 (2016) 158-167.
45. P. Kumar, A. Nagarajan, P.D. Uchil, Analysis of Cell Viability by the MTT Assay, Cold Spring Harbor protocols 2018(6) (2018).
46. W.Y. Wang, M.S. Tan, J.T. Yu, L. Tan, Role of pro-inflammatory cytokines released from microglia in Alzheimer's disease, Ann Transl Med 3(10) (2015) 136.
47. S.H. Choi, E. Bylykbashi, Z.K. Chatila, S.W. Lee, B. Pulli, G.D. Clemenson, E. Kim, A. Rompala, M.K. Oram, C. Asselin, J. Aronson, C. Zhang, S.J. Miller, A. Lesinski, J.W. Chen, D.Y. Kim, H. van Praag, B.M. Spiegelman, F.H. Gage, R.E. Tanzi, Combined adult neurogenesis and BDNF mimic exercise effects on cognition in an Alzheimer's mouse model, Science 361(6406) (2018).
48. C. Anacker, R. Hen, Adult hippocampal neurogenesis and cognitive flexibility - linking memory and mood, Nature reviews. Neuroscience 18(6) (2017) 335-346.
49. E. Lapi, S. Di Agostino, S. Donzelli, H. Gal, E. Domany, G. Rechavi, P.P. Pandolfi, D. Givol, S. Strano, X. Lu, G. Blandino, PML, YAP, and p73 are components of a proapoptotic autoregulatory feedback loop, Molecular cell 32(6) (2008) 803-14.
50. Q. Xiao, Z. Qian, W. Zhang, J. Liu, E. Hu, J. Zhang, M. Li, J. Wang, F. Kong, Y. Li, R. Wang, X. Tan, D. He, X. Xiao, Depletion of CABYR-a/b sensitizes lung cancer cells to TRAIL-induced apoptosis through

YAP/p73-mediated DR5 upregulation, Oncotarget 7(8) (2016) 9513-24.

51. F. Cottini, T. Hideshima, C. Xu, M. Sattler, M. Dori, L. Agnelli, E. ten Hacken, M.T. Bertilaccio, E. Antonini, A. Neri, M. Ponzoni, M. Marcatti, P.G. Richardson, R. Carrasco, A.C. Kimmelman, K.K. Wong, F. Caligaris-Cappio, G. Blandino, W.M. Kuehl, K.C. Anderson, G. Tonon, Rescue of Hippo coactivator YAP1 triggers DNA damage-induced apoptosis in hematological cancers, Nat Med 20(6) (2014) 599-606.
52. M. Xu, D.F. Zhang, R. Luo, Y. Wu, H. Zhou, L.L. Kong, R. Bi, Y.G. Yao, A systematic integrated analysis of brain expression profiles reveals YAP1 and other prioritized hub genes as important upstream regulators in Alzheimer's disease, Alzheimer's & dementia : the journal of the Alzheimer's Association 14(2) (2018) 215-229.
53. F. Yin, J. Yu, Y. Zheng, Q. Chen, N. Zhang, D. Pan, Spatial organization of Hippo signaling at the plasma membrane mediated by the tumor suppressor Merlin/NF2, Cell 154(6) (2013) 1342-55.
54. R. Baumgartner, I. Poernbacher, N. Buser, E. Hafen, H. Stocker, The WW domain protein Kibra acts upstream of Hippo in Drosophila, Developmental cell 18(2) (2010) 309-16.
55. B. Zhao, X. Wei, W. Li, R.S. Udan, Q. Yang, J. Kim, J. Xie, T. Ikenoue, J. Yu, L. Li, P. Zheng, K. Ye, A. Chinnaiyan, G. Halder, Z.C. Lai, K.L. Guan, Inactivation of YAP oncoprotein by the Hippo pathway is involved in cell contact inhibition and tissue growth control, Genes & development 21(21) (2007) 2747-61.
56. J. Dong, G. Feldmann, J. Huang, S. Wu, N. Zhang, S.A. Comerford, M.F. Gayyed, R.A. Anders, A. Maitra, D. Pan, Elucidation of a universal size-control mechanism in Drosophila and mammals, Cell 130(6) (2007) 1120-33.
57. W. Zhang, Y. Gao, F. Li, X. Tong, Y. Ren, X. Han, S. Yao, F. Long, Z. Yang, H. Fan, L. Zhang, H. Ji, YAP promotes malignant progression of Lkb1-deficient lung adenocarcinoma through downstream regulation of survivin, Cancer research 75(21) (2015) 4450-7.
58. S. Strano, O. Monti, N. Pediconi, A. Baccarini, G. Fontemaggi, E. Lapi, F. Mantovani, A. Damalas, G. Citro, A. Sacchi, G. Del Sal, M. Levrero, G. Blandino, The transcriptional coactivator Yes-associated protein drives p73 gene-target specificity in response to DNA Damage, Molecular cell 18(4) (2005) 447-59.
59. M. Howell, C. Borchers, S.L. Milgram, Heterogeneous nuclear ribonuclear protein U associates with YAP and regulates its co-activation of Bax transcription, The Journal of biological chemistry 279(25) (2004) 26300-6.
60. S. Strano, E. Munarriz, M. Rossi, L. Castagnoli, Y. Shaul, A. Sacchi, M. Oren, M. Sudol, G. Cesareni, G. Blandino, Physical interaction with Yes-associated protein enhances p73 transcriptional activity, The Journal of biological chemistry 276(18) (2001) 15164-73.
61. W. Kudo, H.P. Lee, W.Q. Zou, X. Wang, G. Perry, X. Zhu, M.A. Smith, R.B. Petersen, H.G. Lee, Cellular prion protein is essential for oligomeric amyloid-β-induced neuronal cell death, Human molecular genetics 21(5) (2012) 1138-44.

62. F.G. De Felice, P.T. Velasco, M.P. Lambert, K. Viola, S.J. Fernandez, S.T. Ferreira, W.L. Klein, Abeta oligomers induce neuronal oxidative stress through an N-methyl-D-aspartate receptor-dependent mechanism that is blocked by the Alzheimer drug memantine, The Journal of biological chemistry 282(15) (2007) 11590-601.
63. Y. Kitamura, S. Shimohama, W. Kamoshima, T. Ota, Y. Matsuoka, Y. Nomura, M.A. Smith, G. Perry, P.J. Whitehouse, T. Taniguchi, Alteration of proteins regulating apoptosis, Bcl-2, Bcl-x, Bax, Bak, Bad, ICH-1 and CPP32, in Alzheimer's disease, Brain research 780(2) (1998) 260-9.
64. H. Hampel, D. Prvulovic, S. Teipel, F. Jessen, C. Luckhaus, L. Frölich, M.W. Riepe, R. Dodel, T. Leyhe, L. Bertram, W. Hoffmann, F. Faltraco, The future of Alzheimer's disease: the next 10 years, Prog Neurobiol 95(4) (2011) 718-28.
65. E.A. Bignante, N.E. Ponce, F. Heredia, J. Musso, M.C. Krawczyk, J. Millán, G.F. Pigino, N.C. Inestrosa, M.M. Boccia, A. Lorenzo, APP/Go protein Gβγ-complex signaling mediates Aβ degeneration and cognitive impairment in Alzheimer's disease models, Neurobiology of aging 64 (2018) 44-57.
66. D.V. Hansen, J.E. Hanson, M. Sheng, Microglia in Alzheimer's disease, J Cell Biol 217(2) (2018) 459-472.
67. T. Wyss-Coray, J. Rogers, Inflammation in Alzheimer disease-a brief review of the basic science and clinical literature, Cold Spring Harbor perspectives in medicine 2(1) (2012) a006346.
68. Y. Matsuoka, M. Picciano, B. Malester, J. LaFrancois, C. Zehr, J.M. Daeschner, J.A. Olschowka, M.I. Fonseca, M.K. O'Banion, A.J. Tenner, C.A. Lemere, K. Duff, Inflammatory responses to amyloidosis in a transgenic mouse model of Alzheimer's disease, The American journal of pathology 158(4) (2001) 1345-54.
69. R.G. Nagele, M.R. D'Andrea, H. Lee, V. Venkataraman, H.Y. Wang, Astrocytes accumulate A beta 42 and give rise to astrocytic amyloid plaques in Alzheimer disease brains, Brain research 971(2) (2003) 197-209.
70. S. Terzioglu-Usak, Y. Negis, D.S. Karabulut, M. Zaim, S. Isik, Cellular Model of Alzheimer's Disease: Aβ1-42 Peptide Induces Amyloid Deposition and a Decrease in Topo Isomerase IIβ and Nurr1 Expression, Current Alzheimer research 14(6) (2017) 636-644.
71. M.S. Shearman, C.I. Ragan, L.L. Iversen, Inhibition of PC12 cell redox activity is a specific, early indicator of the mechanism of beta-amyloid-mediated cell death, Proc Natl Acad Sci U S A 91(4) (1994) 1470-4.
72. L.J. Zhou, W. Song, X.Z. Zhu, Z.L. Chen, M.L. Yin, X.F. Cheng, Protective effects of bilobalide on amyloid beta-peptide 25-35-induced PC12 cell cytotoxicity, Acta pharmacologica Sinica 21(1) (2000) 75-9.
73. X.Q. Tang, C.T. Yang, J. Chen, W.L. Yin, S.W. Tian, B. Hu, J.Q. Feng, Y.J. Li, Effect of hydrogen sulphide on beta-amyloid-induced damage in PC12 cells, Clinical and experimental pharmacology & physiology 35(2) (2008) 180-6.
74. P.H. Reddy, M.F. Beal, Amyloid beta, mitochondrial dysfunction and synaptic damage: implications for cognitive decline in aging and Alzheimer's disease, Trends in molecular medicine 14(2) (2008) 45-

53.
75. X. Wang, W. Wang, L. Li, G. Perry, H.G. Lee, X. Zhu, Oxidative stress and mitochondrial dysfunction in Alzheimer's disease, Biochimica et biophysica acta 1842(8) (2014) 1240-7.
76. D. Yimlamai, C. Christodoulou, G.G. Galli, K. Yanger, B. Pepe-Mooney, B. Gurung, K. Shrestha, P. Cahan, B.Z. Stanger, F.D. Camargo, Hippo pathway activity influences liver cell fate, Cell 157(6) (2014) 1324-1338.
77. J.L. Grijalva, M. Huizenga, K. Mueller, S. Rodriguez, J. Brazzo, F. Camargo, G. Sadri-Vakili, K. Vakili, Dynamic alterations in Hippo signaling pathway and YAP activation during liver regeneration, American journal of physiology. Gastrointestinal and liver physiology 307(2) (2014) G196-204.
78. T. Su, T. Bondar, X. Zhou, C. Zhang, H. He, R. Medzhitov, Two-signal requirement for growth-promoting function of Yap in hepatocytes, eLife 4 (2015).
79. J. Jin, X. Zhao, H. Fu, Y. Gao, The Effects of YAP and Its Related Mechanisms in Central Nervous System Diseases, Frontiers in neuroscience 14 (2020) 595.
80. H. Tanaka, H. Homma, K. Fujita, K. Kondo, S. Yamada, X. Jin, M. Waragai, G. Ohtomo, A. Iwata, K. Tagawa, N. Atsuta, M. Katsuno, N. Tomita, K. Furukawa, Y. Saito, T. Saito, A. Ichise, S. Shibata, H. Arai, T. Saido, M. Sudol, S.I. Muramatsu, H. Okano, E.J. Mufson, G. Sobue, S. Murayama, H. Okazawa, YAP-dependent necrosis occurs in early stages of Alzheimer's disease and regulates mouse model pathology, Nature communications 11(1) (2020) 507.
81. E.P. Moreno-Jiménez, M. Flor-García, J. Terreros-Roncal, A. Rábano, F. Cafini, N. Pallas-Bazarra, J. Ávila, M. Llorens-Martín, Adult hippocampal neurogenesis is abundant in neurologically healthy subjects and drops sharply in patients with Alzheimer's disease, Nat Med 25(4) (2019) 554-560.

Figures

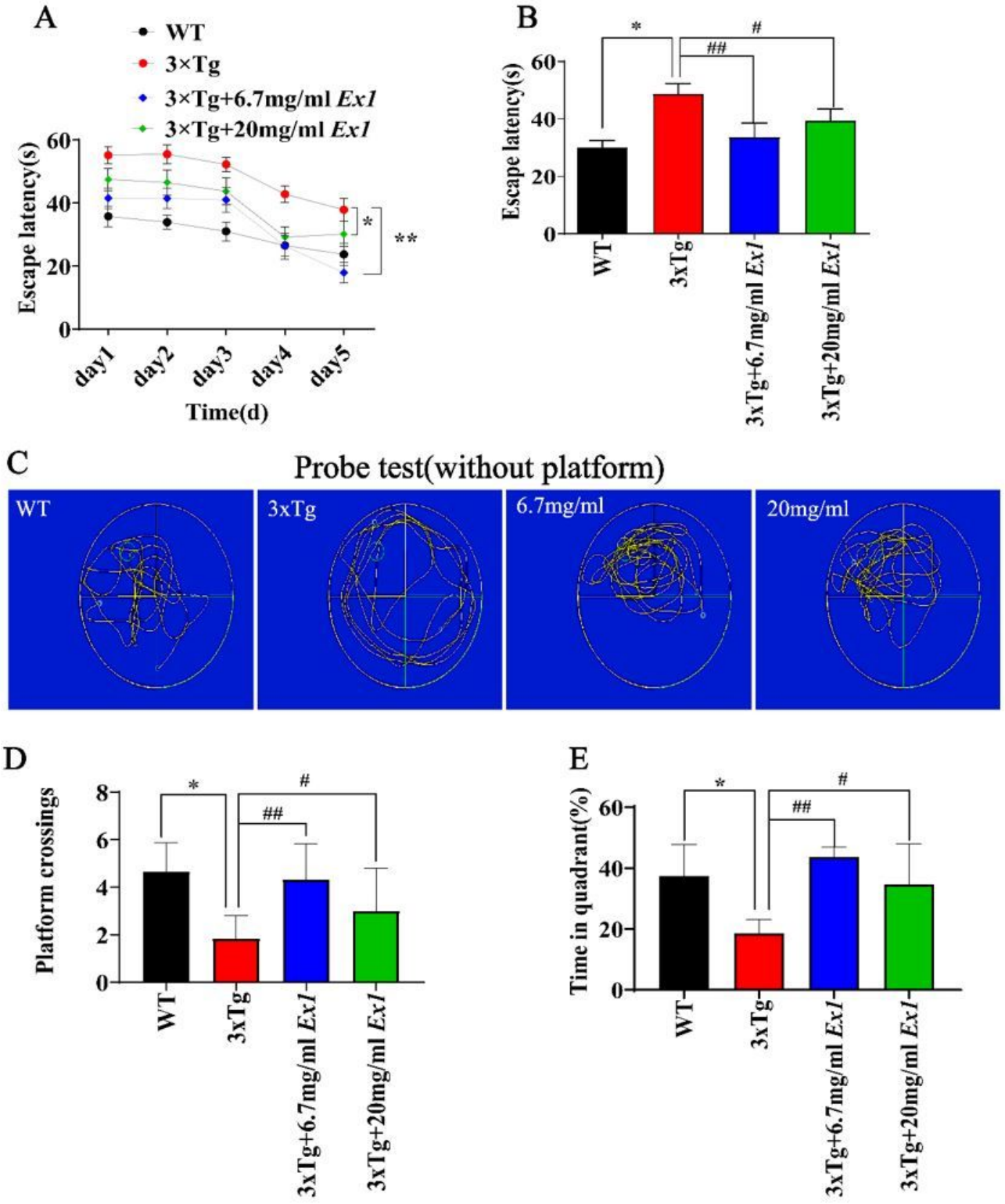

Figure 1

Ex1 improved the behavioral performance of 3xTg AD mice.

Morris water maze test results. (A) Escape latency during platform trials and (B) during spatial probe trial. (C) Representative image of the path of mice in 6 d trials. (D) Quantitative analysis of the number of

platform crossings (E) and of the time spent in the quadrants (Q3, quadrant where the platform is located; o.a. all other quadrants; mean ± SEM, one- or two-way ANOVA, *p < 0.05, **p < 0.01).

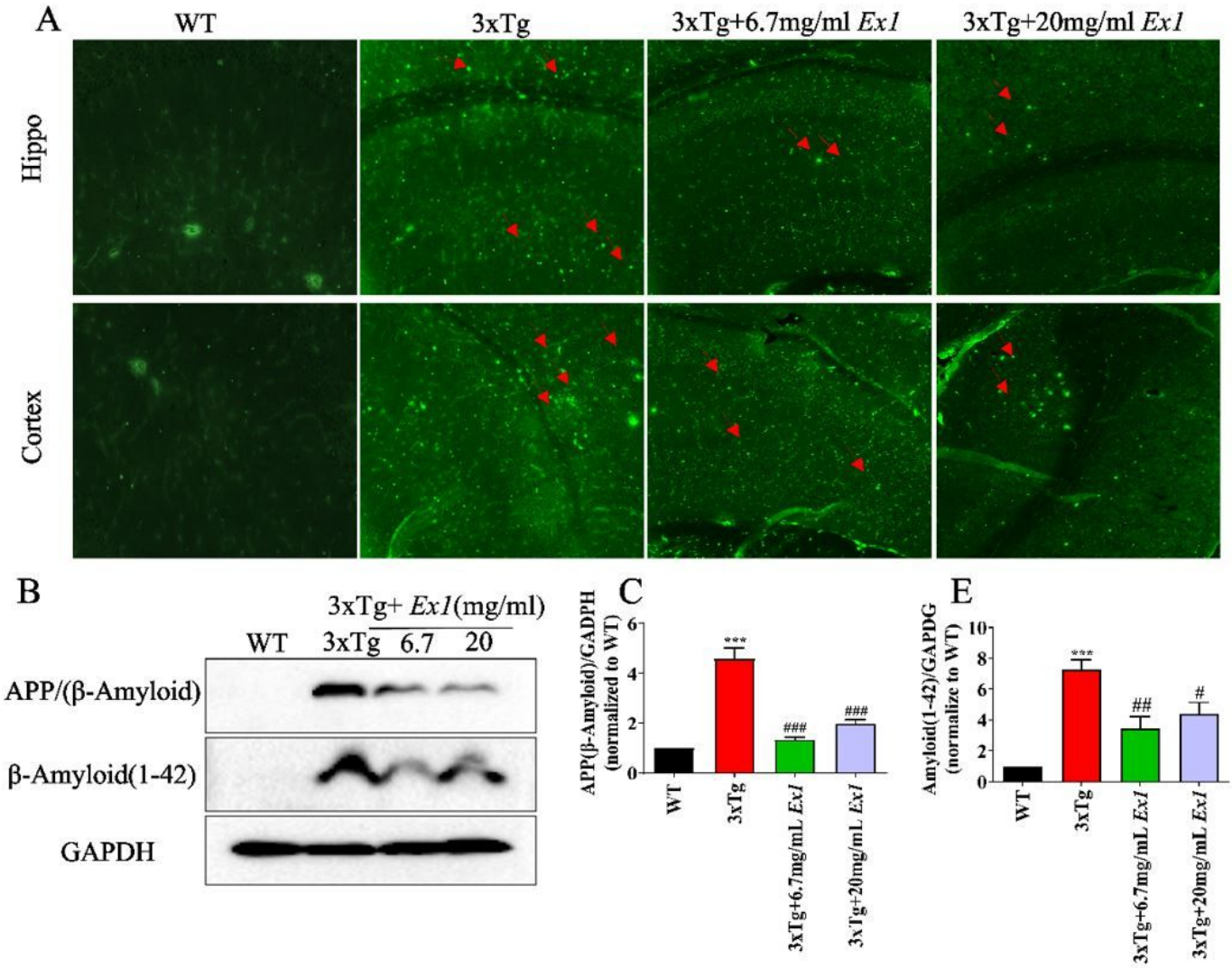

Figure 2

Ex1 ameliorated amyloid deposition in 3xTg AD mice.

(A) Representative images of β-amyloid immunofluorescence staining in different brain areas and (B) quantitative analysis of Aβ area fraction; (C-D) Western blots and quantitative analysis of APP expression levels in brain homogenates. Each experiment was performed in triplicate. *Representative comparison between WT control and 3xTg AD untreated mice, #Representative comparison between 3xTg AD groups, each assay was performed in triplicate. (n=10 per group for brain samples, mean ± SEM, one-way ANOVA followed by Tukey's post-hoc test, *p < 0.05 was considered statisitically significant).

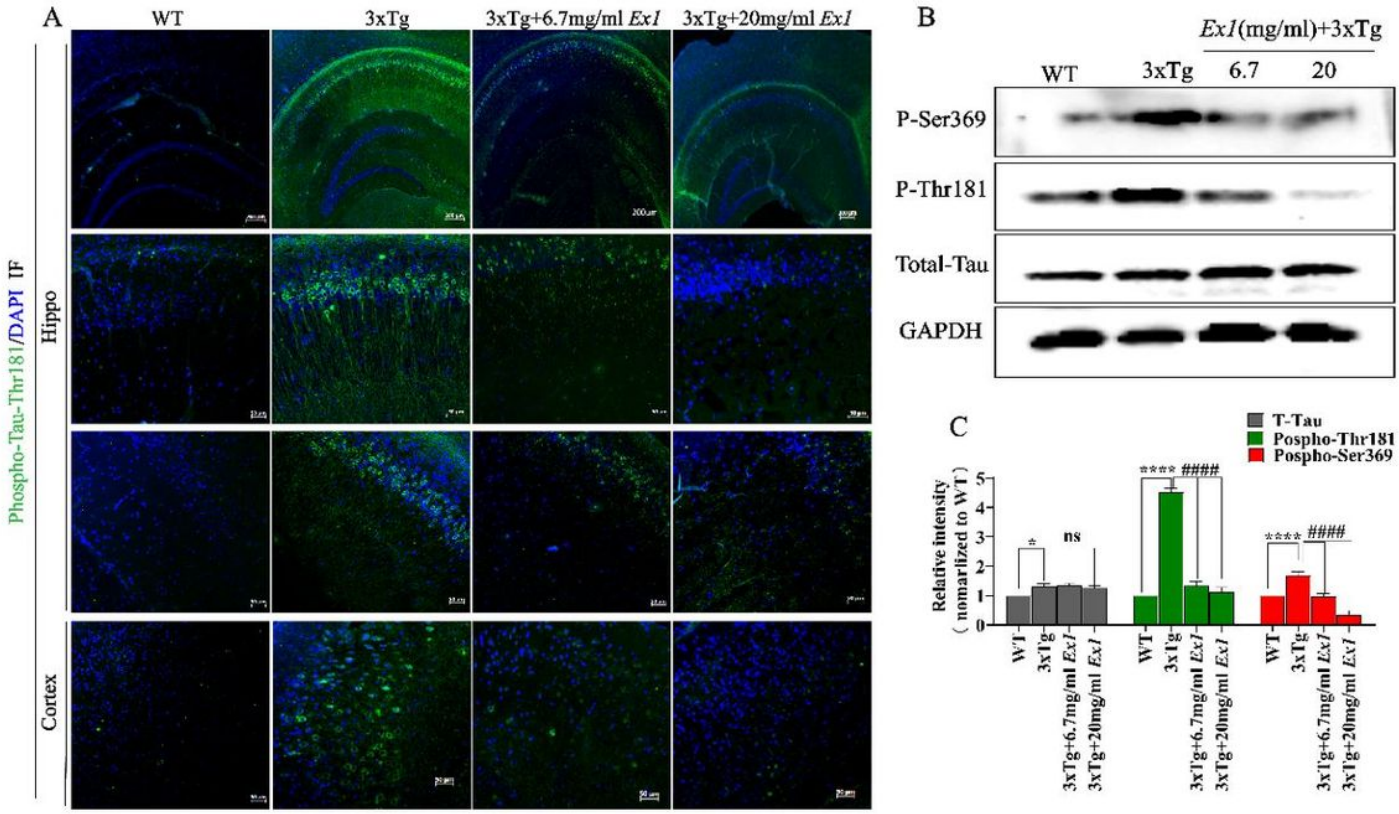

Figure 3

Ex1 reduced Tau-phosphorylation in 3xTg AD mice.

(A) Representative images of phosphorylated Tau immunofluorescence in the hippocampus and cortex of AD mice (scale bars 50 μM)). (B-C) Western blot analysis and quantification of phosphorylated Tau at Ser369-Tau (p-Ser369) and Thr181-Tau (p-Thr181) sites, and total Tau (T-tau) in brain homogenates. (Mean ± SEM, one-way ANOVA followed by Tukey's post-hoc test, *p < 0.05 was considered statistically significant.

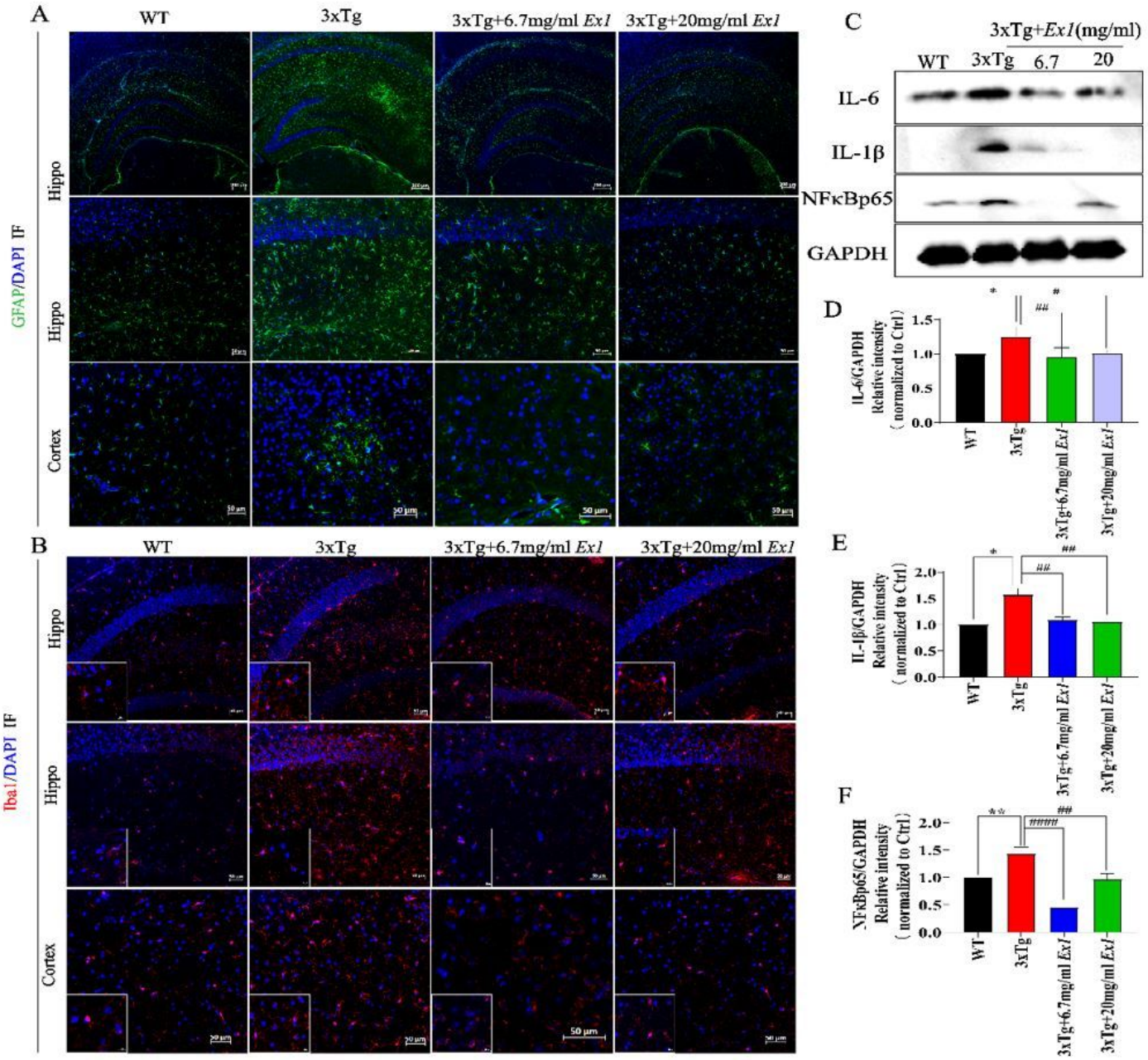

Figure 4

Ex1 attenuated neuroinflammation in 3xTg AD mice.

(A-B) GFAP and Iba-1 immunostaining in the hippocampus and cortex of 3xTg AD-treated and untreated mice (scale bars 50 μM). (C) The expression of the inflammatory factors IL-1β, IL-6, TNF-α and IFN-γ in brain homogenates was detected by Western blot. (D-F) Quantification of C. Each assay was performed in triplicate. *WT-Ctrl vs 3xTg-Ctrl; # 3xTg-Ctrl and different treatment groups, mean± SEM, one-way ANOVA followed by Tukey's post-hoc test, *p < 0.05 was considered statistically significant.

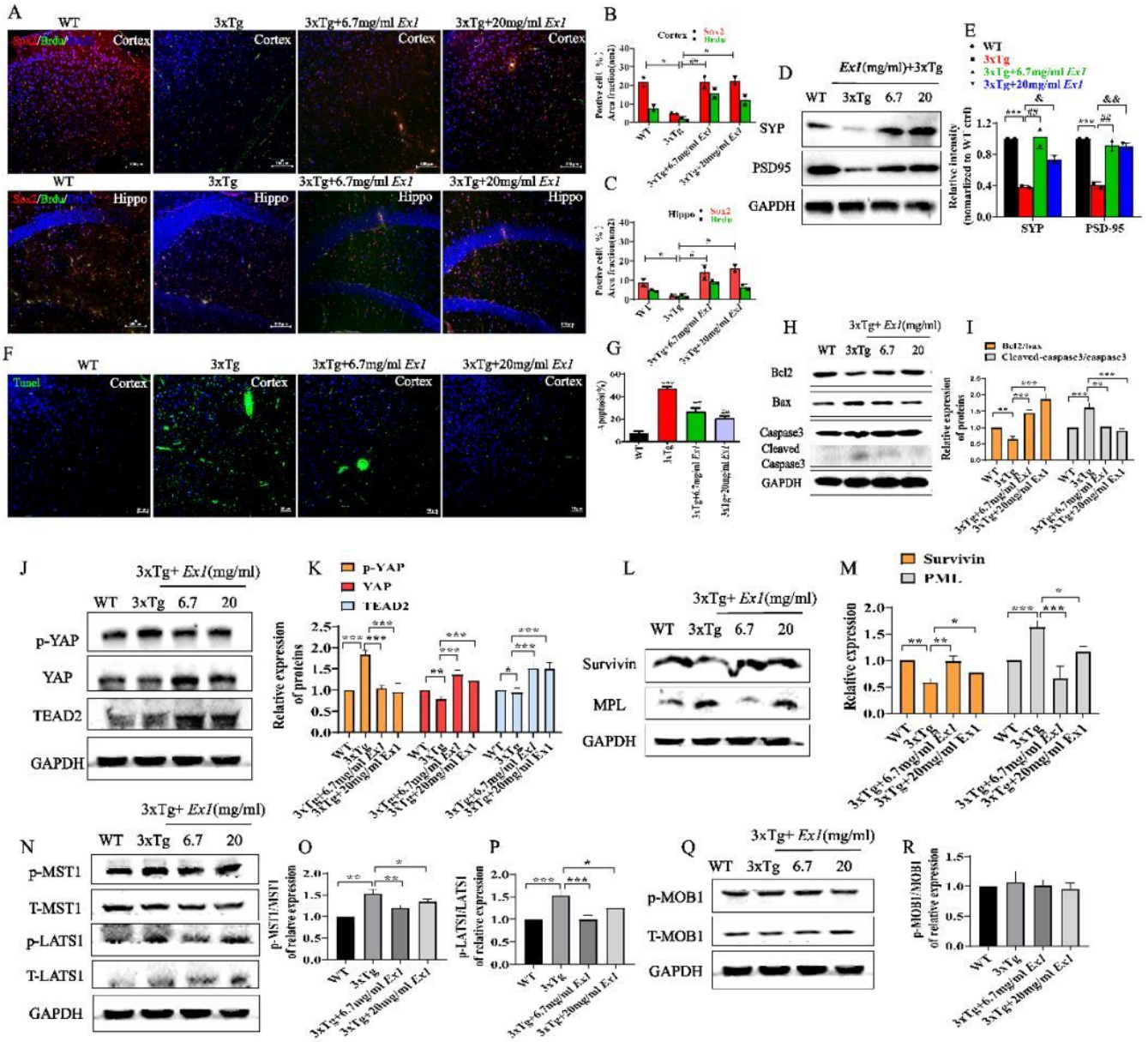

Figure 5

_Ex1_ promoted the proliferation of neural progenitor cells, increased synaptic plasticity, and rescued the neuronal apoptosis in 3xTg mice via regulation of hippo signaling.

(A) Representative images of $Sox2^+$ and $Brdu^+$ in the hippocampus and cortex, (B-C) Quantification of the number of $Sox2^+$ and $Brdu^+$ cells. (D) Western blot analysis of synapse-related protein including synaptophysin (SYP) and PSD95 in brain homogenates. (E) Quantification of D. (F) Apoptosis determined by TUNEL staining in the cortex (scale bars 50 μM). (G) Quantification of F. (H) The expression of Bax, Bcl2, caspase 3 and cleaved caspase-3 and GAPDH was detected by Western blot. (I) Quantification of H. (K) Western blot to assess the expression of p-YAP, YAP, EDTA2, GAPDH. (L) The downstream proteins expression of YAP such as survivin, and PML was detected by western blot. (M) Quantification of L. (N-R) The upstream proteins expression of YAP including p-MST1, MST1, p-LAST1, LAST1, p-MOB1, MOB1 and

GAPDH was assessed by western blot. (*comparison between WT and 3xTg AD mice, #comparison between 3xTg-Ctrl and treatment groups, mean± SEM, Student t test, #/*p < 0.05, ##/**p < 0.01).

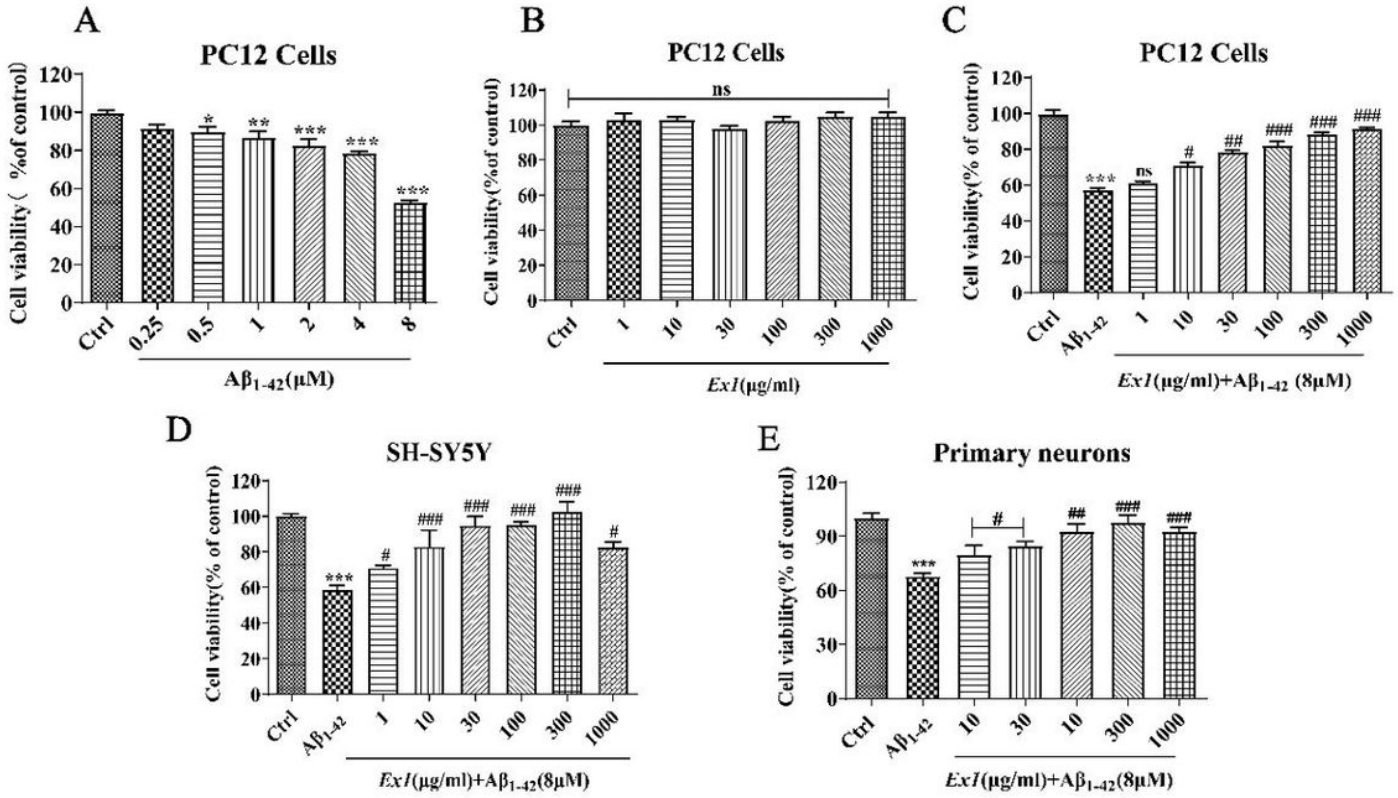

Figure 6

Ex1 reduced the neurotoxicity triggered by $A\beta_{1-42}$.

(A) Assessment of $A\beta_{1-42}$ cytotoxicity. Cells were treated with different concentrations of $A\beta_{1-42}$ (0.5-8 μM) for 24 hours and cell viability was assessed using the MTT assay. ***p<0.001 versus Ctrl group. (B) Assessment of the effect of *Ex1* treatment on $A\beta_{1-42}$-induced neurotoxicity. Cells were incubated with 8 μM $A\beta_{1-42}$ and treated with different concentrations of *Ex1* for 24 hours and cellular viability was assessed using the MTT assay. (C) Assessment of *Ex1* neurotoxicity. Cells were treated with different concentrations of *artemisia annua Ex1* extracts (1~1000 μg/ml) for 24 hours and cell viability was measured using the MTT assay. (D) Cellular viability of SH-SY5Y cells treated with 8 μM $A\beta_{1-42}$ alone or with (30 μg/ml, 100 μg/ml, 300 μg/ml) *Ex1*. (E) Cellular viability of primary neurons treated with 8 μM $A\beta_{1-42}$ alone or with (30 μg/ml, 100 μg/ml, 300 μg/ml) *Ex1*. Each assay was performed in triplicate and the experiment was repeated three times (n = 3, mean ± SEM, one-way ANOVA followed by Tukey's post-hoc test. *p<0.05, **p<0.01, ***p<0.001, were considered statistically significant. *Representative comparison between Ctrl and $A\beta_{1-42,}$ #Representative comparison between $A\beta_{1-42}$ and *Ex1* treatment).

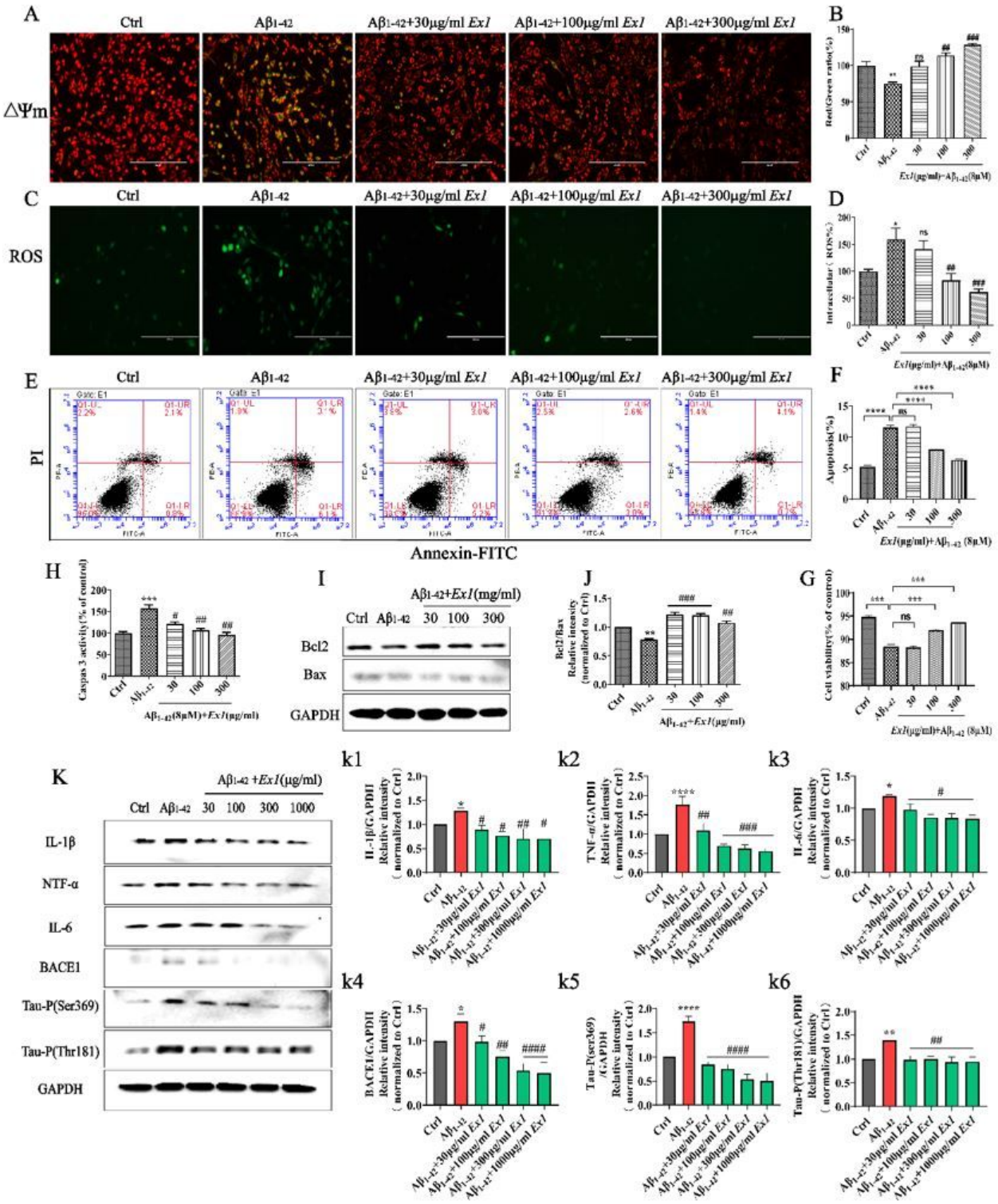

Figure 7

***Ex1* attenuated apoptosis induced by Aβ1-42 and alleviated the pathologic changes triggered by $Aβ_{1-42}$ in PC12 cells.** PC12 cells were treated with 8 μM $Aβ_{1-42}$ alone or with (30 μg/ml, 100 μg/ml, 300 μg/ml) *Ex1*. (A-B) The restoration of the mitochondrial membrane potential was denoted by the shift of red

fluorescence to green indicated by JC-1 staining. (C-D) Intracellular ROS levels were measured by the CellROXs Deep Green Reagent (scale bars 200μm). (E-G) Flow cytometry and quantitative analysis of cellular apoptosis. (H) Caspase 3 was detected by caspase 3 activity test assay kit. (I) Western blot analysis of Bcl-2 and Bax. GAPDH was used as loading control. (J) Quantification of Bcl2/Bax expression from I. (K) Western blot analysis of the pro-inflammatory factors IL-1β, IL-6, TNF-α, the β-site APP cleaving enzyme 1 (BACE1), pS396-Tau and pT181-Tau, and GAPDH expression. (k1-k6) Quantification of K. Each assay was performed in triplicate and the experiment was repeated three times (n = 3, mean ± SEM, one-way ANOVA followed by Tukey's post-hoc test. *$p<0.05$, **$p<0.01$, ***$p<0.001$ were considered statistically significant. *Representative comparison between Ctrl and $A\beta_{1-42}$, #Representative comparison between $A\beta_{1-42}$ and treatment).

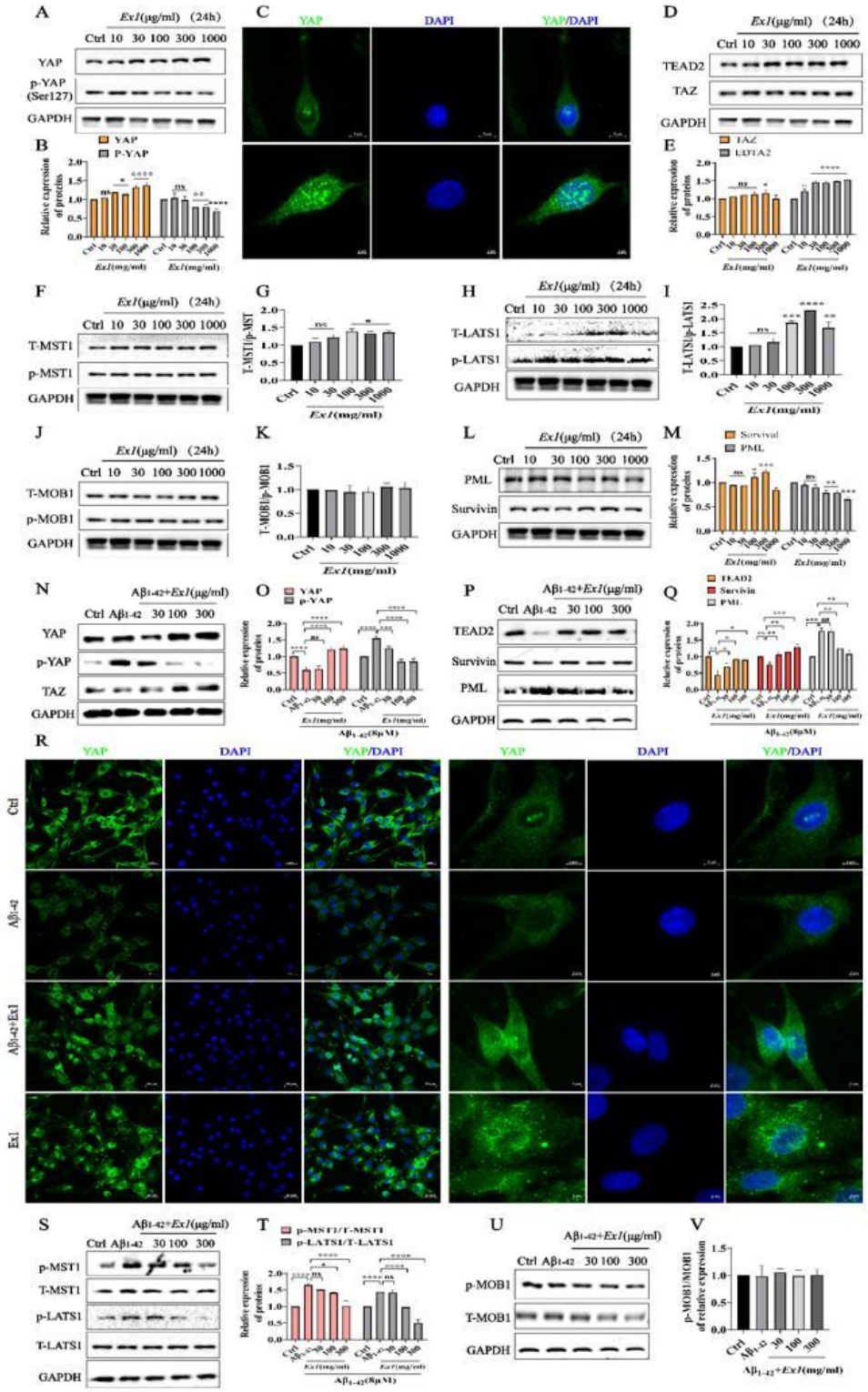

Figure 8

Ex1 protective effect occurs via regulating YAP signaling in PC12 cells.

PC12 cells were treated with (30 μg/ml, 100 μg/ml, 300 μg/ml, 1000 μg/m) *Ex1* for 24 h. (A) Western blot analysis of YAP, P-YAP, and GAPDH expression. (B) Quantification of A, *Ex1* increased the expression of YAP and decreased the phosphorylation of YAP in a dose-dependent manner. (C) Immunofluorescence of

YAP. (D) The expression of TEAD2, TAZ and GAPDH were detected by western blot. (E) Quantification of D, *Ex1* promoted the expression of TEAD2 and TAZ in PC12 cells. (F) Western blot analysis of T-MST1/p-MST1 expression ratio. (G) Quantification of F, *Ex1* increased the expression ratio of T-MST1/p-MST1. (H) Western blot analysis of T-LATS1/p-LATS1 expression ratio. (I) Quantification of H, *Ex1* increased the expression ratio of T-LATS1/p-LATS1. (J) Western blot analysis of T-MOB1/p-MOB1 expression ratio. (K) Quantification of J, *Ex1* increased the expression ratio of T-LATS1/p-LATS1. (L) Western blot analysis of the pro-apoptosis protein PML, anti-apoptosis protein survivin and GAPDH expression. (M) Quantification of L, *Ex1* decresed the expression of PML, and increased the expression of survivin. (N-P) PC12 cells were incubated with 8 μM $A\beta_{1\text{-}42}$ with or without *Ex1* at different concentrations for 24h. Western blot analysis of the effect of *Ex1* on YAP, p-YAP, TAZ, TEAD2, survivin, PML and GAPDH. (O-Q) Quantification of N and P. (R) Immunofluorescence of YAP expression. (S) Western blot analysis of p-MST1/T-MST1 and p-LATS1/T-LATS1 expression ratios. (T) Quantification of S. (U) Western blot analysis of p-MOB1/T-MOB1 expression ratio. (V) Quantification of U. Each assay was repeated in triplicate (Mean ± SEM, one-way ANOVA, Tukey's post-hoc test). *p < 0.05 was considered statistically significant.

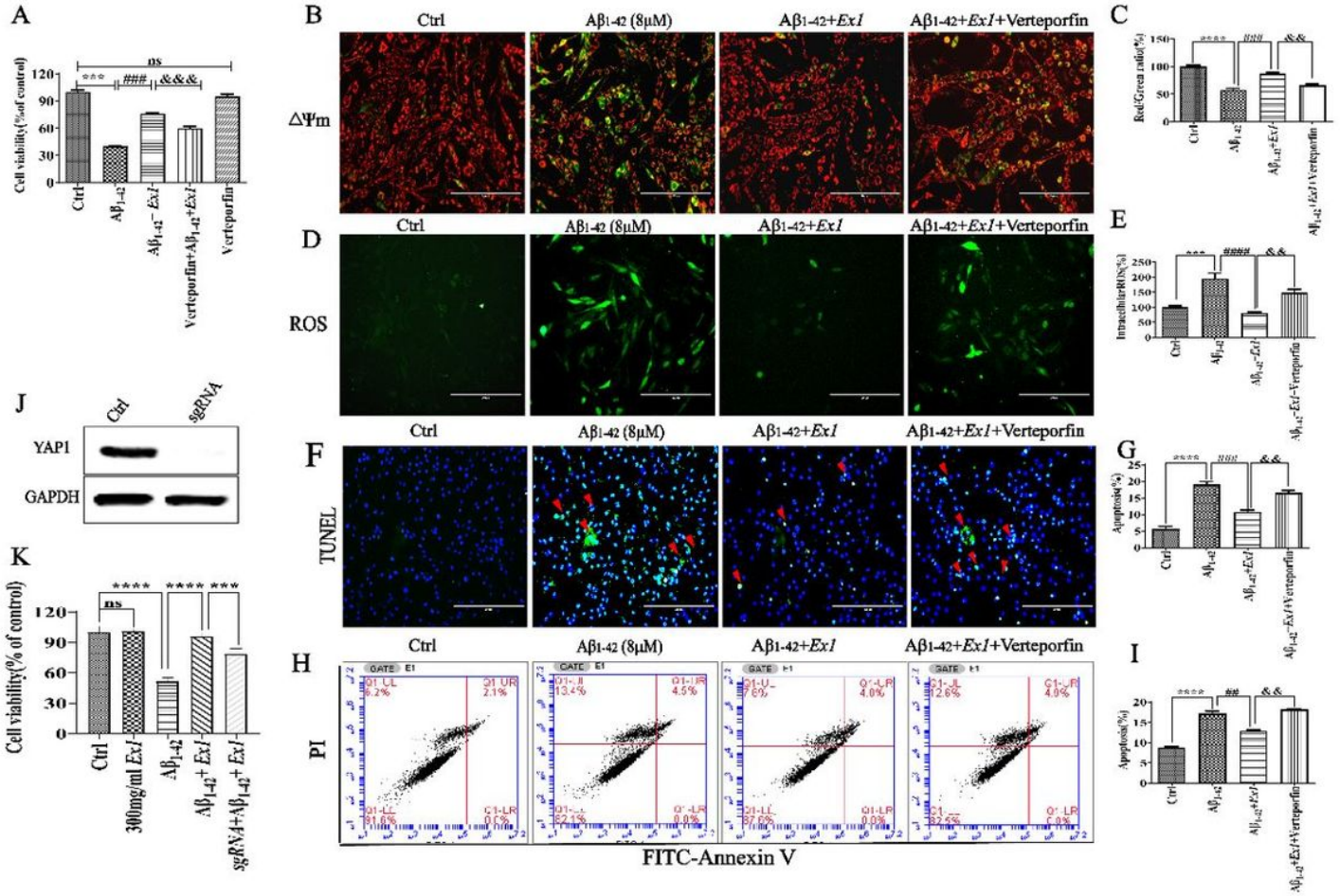

Figure 9

YAP signaling mediated the protective effects of *artemisia annua* extracts in PC12 cells. PC12 cells were pretreated with 2.5 μM Verteporfin (YAP inhibitor) for 60 min and incubated with 8 μM $A\beta_{1-42}$ in the presence or absence of 300 μg/ml *Ex*1. (A) Verteporfin inhibited the protective effect of *Ex1* on $A\beta_{1-42}$ induced neurotoxicity. (B-C) The mitochondrial membrane potential was measured by JC-1 staining (scale bars 200 μM). (D-E) Intracellular ROS levels were measured by ROS assay (scale bars 200 μM). (F-G) Apoptosis was measured by TUNEL staining (scale bars 200 μM). (H-I) Apoptosis was measured by Flow cytometry. (I) Cell viability was measured by MTT assay. (J) Western blotting analysis of YAP expression in WT and KO cells. (K) The viability of cells was measured by MTT assay. Each experiment was repeated in triplicate (n=3, Mean ± SEM, one-way ANOVA, Tukey's post-hoc test). *$p< 0.05$ was considered statistically significant. *Representative comparison between Ctrl and $A\beta_{1-42}$; #Representative comparison between $A\beta_{1-42}$ and *Ex1* treatment; &Representative comparison between $A\beta_{1-42}$ and $A\beta_{1-42}$+*Ex1*+Verteporfin.

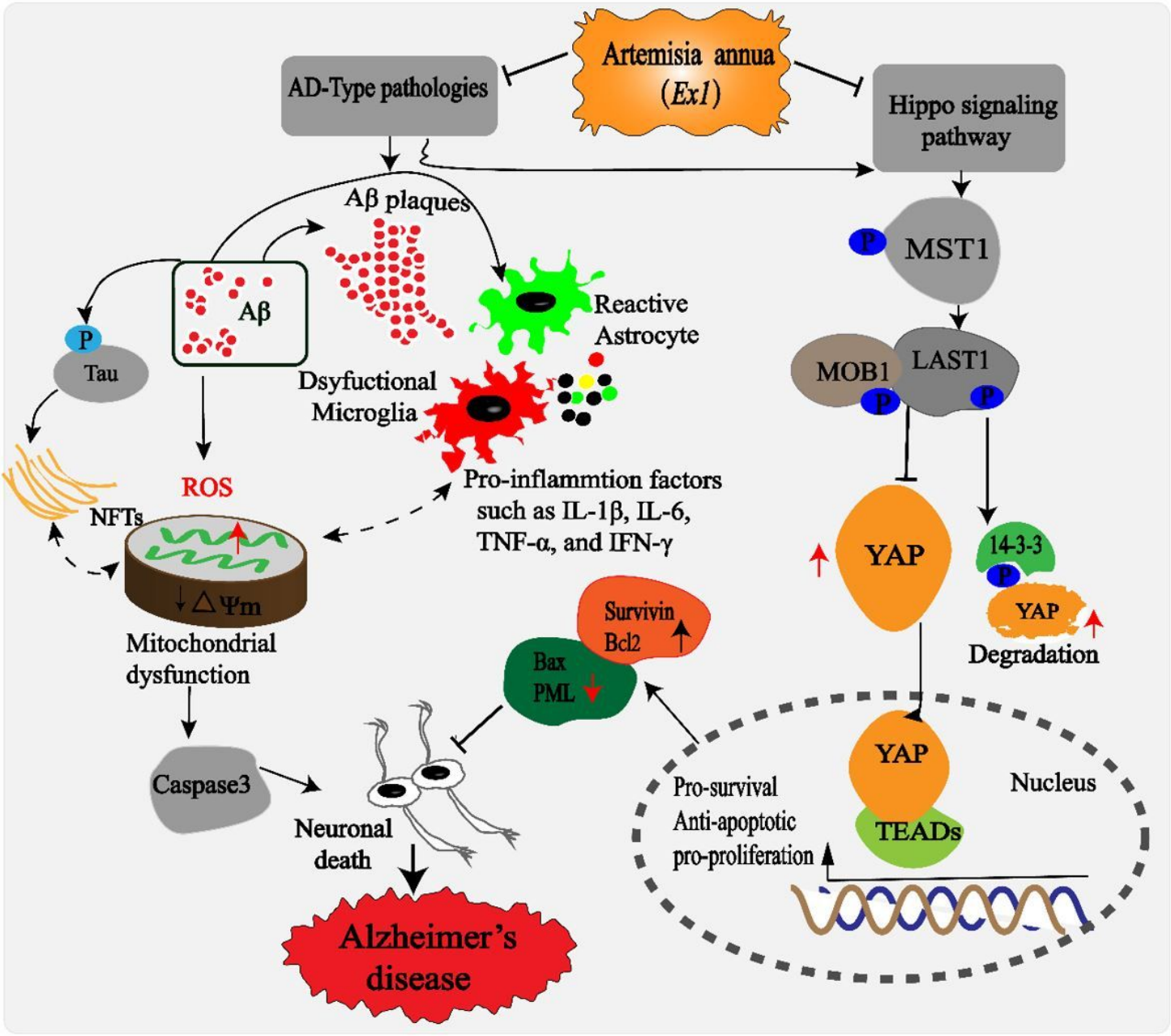

Figure 10

The possible mechanism of *artemisia annua* action on Alzheimer's disease.

Artemisia annua stimulated YAP overexpression in neuronal cells and in the brain of 3xTg mice, resulting in the activation of YAP, survivin/Bcl2 survival pathway and inhibition of apoptosis pathway. This process may inhibit Aβ aggregation and the downstream pathologic events triggered by Aβ such as oxidative stress, mitochondrial dysfunction, Tau phosphorylation and neuroinflammation. *Artemisia annua* may rescue neuronal loss and prompt the functional recovery of AD through YAP/TEADs/survivin.

Supplementary Files

This is a list of supplementary files associated with this preprint. Click to download.

- SupplementaryFigures.docx